Sediment-Water Exchange of Polycyclic Aromatic Hydrocarbons in the Lower Hudson Estuary

by

Rachel G. Adams

B.S. Chemical Engineering
University of Michigan, Ann Arbor, 1994

Submitted to the Department of Civil and Environmental Engineering in Partial Fulfillment of the Requirements of the Degree of

MASTER OF SCIENCE
IN CIVIL AND ENVIRONMENTAL ENGINEERING

at the

MASSACHUSETTS INSTITUTE OF TECHNOLOGY

June 2000

Signature of the Author _____
Department of Civil and Environmental Engineering
May 19, 2000

Certified by _____
Philip M. Gschwend
Professor of Civil and Environmental Engineering
Thesis Supervisor

Accepted by _____
Professor Daniele Veneziano
Chairman, Departmental Committee on Graduate Studies

Sediment-Water Exchange of Polycyclic Aromatic Hydrocarbons in the Lower Hudson Estuary

by

Rachel G. Adams

Submitted to the Department of Civil and Environmental Engineering on May 19, 2000 in partial fulfillment of the requirements for the Degree of Master of Science in Civil and Environmental Engineering

ABSTRACT

Polyethylene devices (PEDs), which rely on the partitioning of hydrophobic organic contaminants (HOCs) between water and polyethylene, were shown to be useful for the measurement of dissolved HOCs like polycyclic aromatic hydrocarbons (PAHs) in natural waters. These PEDs allow for the measurement of the fugacity or "fleeing tendency" of such chemicals in water. These dissolved concentrations are of ecotoxicological concern as they reflect the HOC fraction that is driving uptake by the surrounding organisms. Because PEDs require on the order of days to equilibrate in the field, their use provides time-averaged measurements. Laboratory-measured polyethylene-water partition coefficients for two PAHs were: 17,000 ±1000 (mol/L_{PE})/(mol/L_w) for phenanthrene and 89,000 ± 6000 (mol/L_{PE})/(mol/L_w) for pyrene. These organic polymer-water partition coefficients were found to be comparable to other organic solvent-water partitioning coefficients. These large coefficients allowed for the measurement of dissolved concentrations as low as 1 pg/L for benzo(a)pyrene and 400 pg/L for phenanthrene in the lower Hudson Estuary.

Sampling performed in the lower Hudson Estuary during neap and spring tides revealed increased concentrations of dissolved pyrene and benzo(a)pyrene, but not phenanthrene, during increased sediment resuspension. These data suggest that resuspension events mostly influence the bed-to-water exchange of PAHs with greater hydrophobicities. PAH water concentrations predicted assuming dissolved and sorbed concentrations related via the product, $f_{om}K_{om}$, where f_{om} is the fraction of organic matter in the suspended sediments and K_{om} is the organic-matter-normalized solid-water partition coefficient for the PAH of concern, were far from observed concentrations. Adding the influence of soot to the partition model via $K_d = f_{om}K_{om} + f_{sc}K_{sc}$, where f_{sc} is the weight fraction of soot carbon in the solid phase and K_{sc} is the soot carbon-water partition coefficient estimated form activated carbon data, yielded predicted concentrations that were much closer to the observed values when PAH partitioning to soot was included in the partitioning model. This finding suggests that soot plays an important role in controlling the cycling of PAHs in the aquatic environment. However, even when the soot partitioning of PAHs was included in the model, the predicted dissolved values were still larger than the measured values. This suggests that the time of particle resuspension is too short to allow for particle-water sorptive equilibrium. Using ratios of source indicative PAHs, it was estimated that 90% of the dissolved PAH fraction was derived from petrogenic sources. In contrast, the same source ratios for the total (dissolved and sorbed) PAH concentrations indicated that only 55% of the total were petrogenically-derived. The observations in this work suggest that efforts to regulate and remediate PAH-contaminated sediments must consider the potential impacts of soot associations of the PAHs.

Thesis Supervisor: Dr. Philip M. Gschwend
Title: Professor of Civil and Environmental Engineering

ACKNOWLEDGMENTS

I would like to thank the people who have helped me to complete this work. I thank my advisor, Phil Gschwend, for his enthusiasm and knowledge. He inspired this work with his myriad of insightful ideas and suggestions. None of this would have been possible without him. John MacFarlane has taught me more things in the lab than I can begin to list. He has been incredibly helpful. He was a huge part of the sampling and helped with several of the lab extractions. Most importantly, he has been a joy to work with; I don't know what I would have done without him. Thanks to Terry Donoghue for piloting the *Mytilus* during the Hudson sampling. Sanjay Pahuja has also helped me during field sampling excursions. His great sense of humor has made these sometimes-difficult trips a lot of fun. I have also enjoyed his friendship. Rocky Geyer and Jon Woodruff have taught me a lot about the particle transport in the lower Hudson Estuary. I am thankful to Steve Margulis for allowing me to bounce my ideas off of him and for offering his help and many good ideas in return. He has been so supportive; I don't know what I would do without him. I also want to thank everyone in the Gschwend Lab. Thanks especially to Allison MacKay, Chris Swartz, and Örjan Gustafsson for sharing their knowledge and making me feel welcome in the lab. It's so nice to work with people that are kind and considerate. Finally, I would like to thank all of my friends in the Parsons lab for making my working environment so enjoyable.

I would also like to thank the Office of Naval Research (Grant #'s N00014-93-1-0883 and N00014-99-1-0039) along with the Ralph M.Parsons Foundation for funding this work.

TABLE OF CONTENTS

LIST OF TABLES

LIST OF FIGURES

CHAPTER 1: INTRODUCTION

Improving our understanding of the fate of organic anthropogenic chemicals within the environment is important. This understanding aids in the evaluation of risks imposed by chemicals already in the environment and allows for the prediction of the distribution of chemicals not yet released. For example, if the producers of dichlorodiphenyltrichloroethane (DDT) had predicted that it would bioaccumulate to levels that caused reproductive toxicity threatening the extinction of several bird species (Carson, 1962), they may have produced a pesticide with fewer harmful effects. Studying the transport of anthropogenic chemicals also enhances our understanding of environmental processes. For example, because trichlorofluoromethane (Freon-11) has no natural source, the air-sea distribution of this chemical has been used to study air-sea gas exchange (Liss and Slater; 1974). Researchers must develop quantitative models for the mass transfer kinetics, equilibria, and transformations of chemicals in the environment both on a molecular and macroscopic level. By quantifying the distribution of chemicals in the environment with respect to environmental parameters, and considering the compound-specific properties of each chemical in question, we may gain an improved understanding of the mechanisms governing the fate of these chemicals in the environment (Blumer, 1975; Stumm et al., 1983; Gschwend and Schwarzenbach, 1992).

Historical sedimentary records indicate that anthropogenic activities have been responsible for the introduction of large concentrations of polycyclic aromatic hydrocarbons (PAHs) into the environment over the last 100 years (Grimmer and Böhnke, 1977; Prahl and Carpenter, 1979; Gschwend and Hites, 1981). PAHs are compounds of environmental and human health concern as

many are toxic, and several have been found to be mutagenic or carcinogenic (Miller and Miller, 1981; Jacob et al., 1986). Many PAHs are produced through the combustion of fossil fuel and wood and carried through the air on particles; much of this load is removed from the atmosphere through rain or dry fallout. PAHs may also be introduced directly to the environment through petroleum spills. Many are washed into water bodies where they are deposited into the sediments (Farrington et al., 1976; Gschwend and Hites, 1981).

Once in the aquatic environment, the hydrophobic nature of these contaminants (e.g., PAHs, polychlorinated biphenyls) causes them to be strongly associated with sediments. In fact, even after the inputs of hydrophobic organic contaminants (HOCs), including PAHs, are reduced or discontinued, the sediments may still be a large source of these pollutants to the overlying waters. Recent studies (Flores, 1998, Petroni and Israelsson, 1998) indicate that the sediments in Boston Inner Harbor are responsible for between 40 and 100% of the PAHs present in the water column. Similarly, Achman (1996) found the sediments to be the dominant source of polychlorinated biphenyls (PCBs) to the lower Hudson River.

In order to understand and predict the speciation of PAHs between the dissolved and sorbed phase, one must be able to measure the concentration of these chemicals in each of these phases. Until recently, measuring the concentrations of HOCs that are dissolved has required the extraction of large volumes of water due to the generally low dissolved concentrations of HOCs. This water must also be filtered in order to remove particulate matter; however, depending on the size of filter used, colloids and even larger particles may still be present in the "dissolved" or filtered portion of the sample. The preferential partitioning of HOCs (e.g., PAHs) onto nonaqueous solids such as

polyethylene allows for the measurement of the fugacity or "fleeing tendency" of such chemicals in water. This fugacity measurement reflects the HOC fraction that is "truly dissolved." It is an indicator of the chemical activities felt by organisms that may either degrade the compounds or experience undesirable toxic accumulations.

The primary objective of this thesis was to further the understanding of the sediment-water exchange of polycyclic aromatic hydrocarbons. In order to accomplish this, the following goals were pursued: (1) develop a polyethylene sampler for measuring the dissolved fraction of hydrophobic organic contaminants (e.g., PAHs) in the environment, and (2) elucidate the processes controlling the distribution of PAHs between the sediments and the water column.

Developing the samplers or polyethylene devices (PEDs) required laboratory experiments for the measurement of the kinetic and equilibrium partitioning of PAHs onto polyethylene. In order to further the understanding of the fate of sediment-sorbed PAHs, hydrographic parameters as well as PAH concentrations (both dissolved and sorbed) were measured in the lower Hudson Estuary. These measurements were then interpreted with respect to existing models in order to gain insight into the processes governing the fate and distribution of these aromatic hydrocarbons.

REFERENCES

Achman, D. R., B. J. Brownawell, and L. Zhang. Exchange of polychlorinated biphenyls between sediment and water in the Hudson River estuary. *Estuaries* **19**, 950-965.

Blumer, M. 1975. Organic compounds in nature: limits of our knowledge. *Angew.Chem. Int. Ed. Engl.* **14**, 507-514.

Carson, R. 1962. *Silent Spring*; Houghton Mifflin, Boston. 368 pp.

Farrington, J. W., N. M. Frew, P. M. Gschwend, and B. W. Tripp. 1977. Hydrocarbons in cores of northwestern Atlantic coastal and continental margin sediments. *Estuarine and Coastal Marine Science* **5**, 793-808.

Flores, A. E. 1998. Assessing the Fate of PAHs in the Boston Inner Harbor Using Semipermeable Membrane Devices (SPMDs). Master of Engineering Thesis. Dept. of Civil and Environmental Engineering. MIT. 121 pp.

Grimmer, G. and H Böhnke. 1977. Investigations of drilling cores of sediments of Lake Constance. I. Profiles of the polycyclic aromatic hydrocarbons. *A. Naturforsch.* **32c**. 703-711.

Gschwend, P. M. and R. A. Hites. 1981. Fluxes of polycyclic aromatic hydrocarbons to marine and lacustrine sediments in the northeastern United States. *Geochim. Cosmochim. Acta* **45**, 2359-2367.

Gschwend, P. M. and R. P. Schwarzenbach. 1992. Physical chemistry of organic compounds in the marine environment. *Marine Chemistry* **39**, 187-207.

Jacob, J., W. Karcher, J. J. Belliardo, and P. J. Wegstaffe. 1986. Polycyclic aromatic hydrocarbons of environmental and occupational importance. *Fresenius, Z. Anal. Chem.* **323**, 1-10.

Liss, P.S. and P. G. Slater. 1974. Flux of gases across the air-sea interface. *Nature* **247**, 181-184.

Miller, E. C. and J. A. Miller. 1981. Searches for ultimate chemical carcinogens and their reactions with cellular macromolecules. *Cancer* **47**, 477-481.

Petroni, R. N. and P. H. Israelsson. 1998. Mass Balance and 3D Model of PAHs in Boston's Inner Harbor. Master of Engineering Thesis. Dept. of Civil and Environmental Engineering. MIT. 224 pp.

Prahl, F. G. and R Carpenter. 1979. The role of zooplankton fecal pellets in the sedimentation of polycyclic aromatic hydrocarbons in Dabob Bay, Washington. *Geochim. Cosmochim. Acta* **43**, 1959-1972.

Stumm, W., R. Schwarzenbach, and L. Sigg. 1983. From environmental analytical chemistry to ecotoxicology—A plea for more concepts and less monitoring and testing. *Angew. Chem. Int. Ed. Engl.* **22**, 380-389.

CHAPTER 2: POLYETHYLENE DEVICES (PEDS): NEW SAMPLERS FOR MEASURING DISSOLVED HYDROPHOBIC ORGANIC CONTAMINANTS IN WATER

INTRODUCTION

In order to study the fate and distribution of hydrophobic organic contaminants (HOCs) in the environment, it is important to measure not only the concentrations of these chemicals sorbed to particles, but more importantly, the concentrations that are dissolved and therefore more readily bioavailable. Until recently, measuring the concentrations of HOCs that are dissolved has required the extraction of large volumes of water due to the low dissolved concentrations of HOCs. This water must also be filtered in order to remove particulate matter; however, depending on the size of filter used, colloids and even larger particles may still be present in this "dissolved" fraction.

The use of polyethylene devices (PEDs), which rely on the partitioning of HOCs between water and polyethylene, allows for the measurement of the fugacity or "fleeing tendency" of a chemical in water. Greater fugacities will result in a larger transfer of chemical into the PED. The fugacities of a chemical in the water are the same fugacities that will be experienced by the biota living in this water. For example, a fraction of the dissolved HOCs may be complexed with colloids and unable to partition into the PED or biota. The fugacity measured with the PED reflects the HOC fraction that is immediately bioavailable or truly dissolved, which is a greater ecotoxicological concern than complexed or sorbed fractions. The use of PEDs will allow us to estimate the dissolved concentration of HOCs and, more importantly, measure the readily bioavailable fraction of HOCs in the water.

In the 1960's the bioaccumulation of organic contaminants, such as dichlorodiphenyltrichloroethane (DDT), in fish and larger animals higher on the food chain became widely recognized (Carson, 1962). In the 1970's scientists began Mussel Watch (Farrington et al., 1983), a program where the concentrations of pollutants in mussels were measured in order to monitor the quality of the waters in which the mussels lived. Because mussels concentrate chemicals by up to factors of 10^5 depending on the chemical, a much smaller sample can be analyzed than could be if the water were extracted. However, differences in biological or biochemical activities of the mussels were believed to result in some of the temporal fluctuations observed in the mussel data. Huckins et al. (1993) developed lipid-containing polyethylene tubes called semipermeable membrane devices (SPMDs) to passively monitor the concentration of HOCs dissolved in the water. These samplers limited variability due to biological activity with the exception of organisms that may grow on the exterior of the membrane. However, many sampling difficulties still exist. SPMDs can tear in the field resulting in a loss of an unknown quantity of the lipid inside, and making it difficult to calculate the HOC concentration that was in the water. Separating the lipid from the HOC can be difficult. Finally, the devices require several weeks to equilibrate with the surrounding waters.

In order to reduce these problems, we have developed a new sampling device. PEDs, which are strips of polyethylene, provide a simple and effective way to measure the concentration of HOCs, such as polycyclic aromatic hydrocarbons (PAHs), dissolved in water and most readily bioavailable. If tearing occurs, this is not a problem as there is no triolein to leak out. Also, the single layer of plastic allows for faster equilibration times. This enables environmental

observations to be made in shorter times. It also results in less time for the formation of biofilms. Finally, the cleanup of the extracts is simplified.

By equilibration of the PEDs with the dissolved fraction of HOCs and looking at the chemical signal, it may be possible to determine the source of this bioavailable fraction. For example, it has been hypothesized that petroleum hydrocarbons discharged to coastal areas are available for biological uptake to a greater extent than pyrogenic hydrocarbons (Farrington et al., 1983). The pyrogenic hydrocarbons are believed to be more strongly associated with pyrogenic particles and less bioavailable than petroleum hydrocarbons. PEDs provide an excellent method to test this hypothesis, as those PAHs that are bioavailable would be expected to diffuse into the PED. The ratios of PAHs present in the PED could then be compared to both petrogenic and pyrogenic source PAH ratios.

The objective of this work was to describe the theory behind PEDs, present the polyethylene-water partition coefficients (K_{PE}) for phenanthrene and pyrene and their diffusivity values in polyethylene, and suggest applications for PED use. These K_{PE} and diffusivity values allow one to calculate the concentrations of dissolved phenanthrene, a three-ringed PAH, and pyrene, a four-ringed PAH, in the water once these PAHs have been measured in the PED.

THEORY

Diffusion in Polyethylene

When a plane sheet is suspended in a large volume of solution such that the amount of solute taken up by the sheet is a negligible fraction of the total solute mass, the concentration in the solution remains constant (Crank, 1975). This is the case for a PED in a large body of water (e.g. a lake, river, harbor, etc.). However, a limited volume of solution will result in a decrease in the concentration of solute in the solution because a significant fraction of solute will diffuse into the plane sheet. The uptake rate varies as a function of the percentage of total chemical finally taken up by the sheet (Figure 2.1; Crank, 1975). The time for uptake increases as the size of the water body increases. For example, the zero curve in Figure 2.1 represents an infinite bath which would be the case at most environmental sampling sites (i.e., lakes, rivers, harbors, etc.).

The limited volume case allows one to measure the change in concentration in the solution over time. The results can be used to estimate the diffusivity of the solute in the sheet. Once the diffusivity is estimated, it can be used to solve for the dissolved concentration of solute in the large volume case. Crank (1975) solved Fick's second law for the diffusion of a chemical from a stirred solution of limited volume into a plane sheet:

$$\frac{M_t}{M_\infty} = 1 - \sum_{n=1}^{\infty} \frac{2\alpha(1+\alpha)}{1+\alpha+\alpha^2 q_n^2} \exp\left(-Dq_n^2 t / l^2\right) \qquad (2.1)$$

where

M_t : the total amount of chemical in the sheet at time t

M_∞: the total amount of chemical in the sheet after an infinite time

D: diffusion coefficient (L^2/T)

T: time (T)

l: length (L)

and the values of q_n are the non-zero positive roots of

$$\tan(q_n) = -\alpha \cdot q_n \tag{2.2}$$

and α is the ratio of the volumes of solution and sheet divided by the partition coefficient:

$$\alpha = \frac{(V_W / V_{PE})}{K_{PE}} \tag{2.3}$$

and K_{PE} [$(M/L^3)/(M/L^3)$] is the polyethylene-water partition coefficient:

$$K_{PE} = \frac{C_{PE}}{C_w} \tag{2.4}$$

The remaining parameters are:

V_W: the volume of water (L^3)

V_{PE}: the volume of polyethylene (L^3)

C_{PE}: the equilibrium concentration of solute in polyethylene (M/L^3)

C_W: the equilibrium concentration of solute in water (M/L^3)

Alpha (α) may also be defined as $(1/f) - 1$, where *f* is the fractional uptake of the sheet. For example, if 50 percent of the chemical initially in the solution is in the sheet at equilibrium, *f* is 0.5, and α is 1. Equation (2.1) can be used to estimate *D* by solving for its best fit with experimental data.

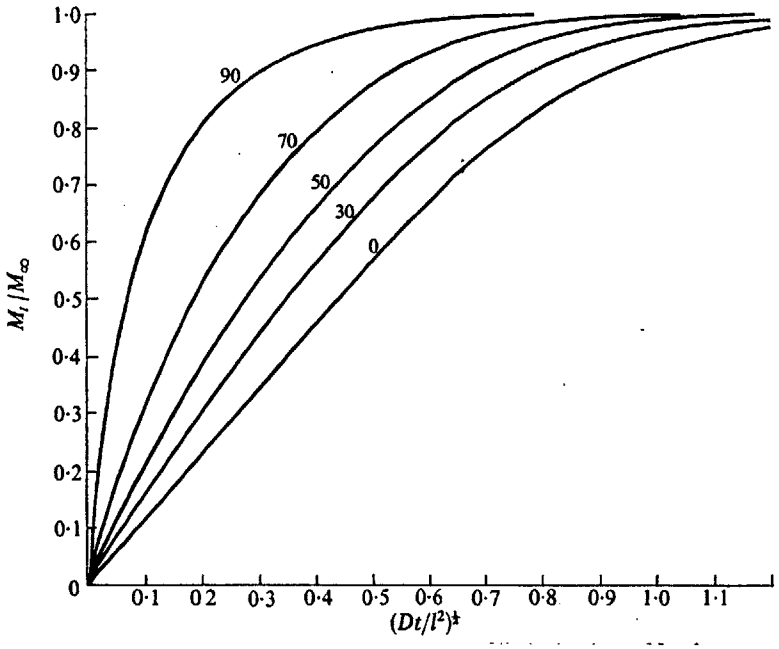

Figure 2.1. Uptake by a plane sheet from a stirred solution of limited volume.

Numbers on curves show the percentage of total solute finally taken up by the sheet. M_t is the total amount of chemical in the sheet at time t, while M_∞ is the total amount of chemical in the sheet after an infinite time. The diffusion coefficient is D (L^2/T), t (T) is time, and l (L) is one-half of the sheet thickness (Crank, 1975).

Water-Dissolved Concentration

When there is an infinite amount of solute or an infinite bath, the following equation, also from Crank (1975), can be used to solve for M_t/M_∞:

$$\frac{M_t}{M_\infty} = 1 - \sum_{n=0}^{\infty} \frac{8}{(2n+1)^2 \pi^2} \cdot \exp\left\{ -D\left(n+\frac{1}{2}\right)^2 \cdot \frac{\pi^2 t}{l^2} \right\} \tag{2.5}$$

The reader is referred to Crank (1975) for a complete discussion of diffusion in a plane sheet. Multiplying both sides of Equation (2.5) by M_∞, dividing both sides by V_{PE}, and substituting C_{PE} for M/V_{PE} results in the following equation:

$$C_{PE@t} = \left[1 - \sum_{n=0}^{\infty} \frac{8}{(2n+1)^2 \pi^2} \cdot \exp\left\{ -D\left(n+\frac{1}{2}\right)^2 \cdot \frac{\pi^2 t}{l^2} \right\} \right] \cdot C_{PE@equilibrium} \tag{2.6}$$

Substituting for $C_{PE@equilibrium}$ from Equation (2.4) and rearranging, one can solve for C_w as a function of C_{PE}, K_{PE}, D, t, and l.

$$C_w = \frac{C_{PE}}{K_{PE} \cdot \left[1 - \sum_{n=0}^{\infty} \frac{8}{(2n+1)^2 \pi^2} \cdot \exp\left\{ -D\left(n+\frac{1}{2}\right)^2 \cdot \frac{\pi^2 t}{l^2} \right\} \right]} \tag{2.7}$$

As t approaches infinity, C_w approaches C_{PE}/K_{PE}. Diffusivity and K_{PE} can be estimated with lab experiments; and C_{PE}, t and l can be measured allowing us to solve for C_w in an infinite bath.

Partition Coefficient

In order to solve Equation (2.7) for the concentration of chemical present in the water, the polyethylene-water partition coefficient needs to be measured. Lab experiments allowed for the

determination of the fraction of chemical present in the water at equilibrium. Assuming that the chemical is present only in the water or the PED (i.e., there are no wall effects), the following equation (Schwarzenbach et al., 1993) gives the fraction of the chemical in the water as a function of the partition coefficient:

$$f_w = \frac{1}{1 + r_{PEW} \cdot K_{PE}} \tag{2.8}$$

where r_{PEW} is the polyethylene-to-water phase ratio, and K_{PE} is the polyethylene-water partition coefficient. Solving Equation (2.8) for K_{PE}, results in the following equation:

$$K_{PE} = \frac{(1/f_w) - 1}{r_{PEW}} \tag{2.9}$$

This equation can be used to solve for the chemical's polyethylene-water partition coefficient.

Time-Dependent Diffusivity

Crank's solution for M_t/M_∞ assumes that diffusivity is constant. In reality, this may not be a good assumption. For example, in polymers, diffusivity is often a function of concentration. As more of the solute diffuses into the membrane, it may cause physical changes in the membrane which then affect diffusivity. Diffusivity may also be a function of distance. The polymer may not be homogenous along the diffusion pathway. For example, the outer layer may be less permeable than the inside of the membrane. Lab experiments, which will be discussed in the following section, indicated that diffusivity was increasing in time and that the constant diffusivity assumption may be poor for the chemicals used in this study, especially pyrene. It appeared that diffusivity may be dependent on concentration or distance. Because both concentration and distance are increasing with time, a solution for time-dependent diffusion coefficients outlined by Crank (1975) was used

to examine this. Finding an increase in diffusivity with increasing time would support the theory that the diffusion coefficient was a function of concentration, distance, or possibly both. Assuming that diffusion is a function of only time results in the following equation:

$$\frac{\partial C}{\partial t} = D(t)\frac{\partial^2 C}{\partial x^2} \tag{2.10}$$

One can then define a new time variable, T, such that:

$$dT = D(t)dt \tag{2.11}$$

Using this transformation, Equation (2.10) becomes

$$\frac{\partial C}{\partial T} = \frac{\partial^2 C}{\partial x^2} \tag{2.12}$$

This is now mathematically equivalent to Equation (2.10) with a coefficient of one on the right hand side. This allows for the use of the Crank solution for Equation (2.1). *D(t)* is defined as the following so that a trend in *D* may be observed.

$$D(t) = \begin{cases} D_1 & 0 < t < t_1 \\ D_2 & t_1 < t < t_2 \\ D_3 & t_2 < t < t_3 \end{cases} \tag{2.13}$$

Taking the integral of Equation (2.11):

$$T = \int_0^t D(t')dt' \tag{2.14}$$

and substituting *D(t)* into Equation (2.14), T becomes

$$T = \begin{cases} D_1(t-0) & 0 < t < t_1 \\ D_2(t-t_1) + D_1 t_1 & t_1 < t < t_2 \\ D_3(t-t_2) + D_2(t_2 - t_1) + D_1 t_1. & t_2 < t < t_3 \end{cases} \tag{2.15}$$

Substituting *T* for *t* in Equation (2.1) results in the following:

$$\frac{M_t}{M_\infty} = \begin{cases} 1 - \sum_{n=1}^{\infty} \beta_n \cdot \exp[-q_n^2 D_1 t / l^2] & 0 < t < t_1 \\ 1 - \sum_{n=1}^{\infty} \beta_n \cdot \exp[-q_n^2 \{D_2(t - t_1) + D_1 t_1\} / l^2] & t_1 < t < t_2 \\ 1 - \sum_{n=1}^{\infty} \beta_n \cdot \exp[-q_n^2 \{D_3(t - t_2) + D_2(t_2 - t_1) + D_1 t_1\} / l^2] & t_2 < t < t_3 \end{cases} \quad (2.16)$$

where

$$\beta_n = \frac{2\alpha(1+\alpha)}{1+\alpha+\alpha^2 q_n^2} \quad (2.17)$$

EXPERIMENTAL SECTION

Experimental Setup

Strips of low-density (0.92 g/cm^3) polyethylene manufactured by Brentwood Plastics, Inc., Brentwood, MO, measuring 2.5 cm wide, 43 cm long, and between 74 and 84 μm thick, were used in the laboratory experiments. Higher density polyethylene has more linear chains with smaller branching ratios (CH_3/1000 CH_2; Miller, 1965). They are more ordered and more crystalline. Lower density polyethylene has larger branching ratios, which result in a larger fraction of non-crystalline or amorphous polymer. In general the more crystalline the polymer, the slower the diffusion of penetrants. Low-density polyethylene has a density ranging from 0.915 to 0.930 g/ml and is between 40 and 50 percent crystalline, while high-density polyethylene density ranges from 0.950 to 0.960 g/ml and is 75 to 90 percent crystalline (Simond and Church, 1963).

Prior to use, each polyethylene strip was extracted with 500 mL of methylene chloride in order to remove any hydrophobic chemicals that may have been absorbed. The polyethylene was allowed

to dry in a laminar flow hood for a minimum of six hours. PEDs that had not been used in the laboratory experiments were extracted in order to measure possible contamination from the vapor phase. One polyethylene device (PED) was to be placed in each of two 10.9 L stainless steel beakers with stainless steel lids (Polar Ware, Sheboygan, WI). These beakers were filled with 10 L of water. The phenanthrene and pyrene were added via methanol solutions purchased in 5000 μg/L and 1000 μg/L concentrations from Supelco (Bellefonte, PA). The resulting beaker concentrations were: 160 μg/L for phenanthrene and 20 μg/L for pyrene. No PED was added to the third beaker, which served as a control. The water was reverse osmosis pretreated and run through an ion-exchange resin and activated carbon filter system (Aries Vaponics, Rockland, MA) until a resistance of 18 MΩ was achieved. The water was then treated with ultraviolet light (Aquafine TOC reduction unit, Valencia, CA) and filtered with a 0.22 μm filter (Millipore). The beaker solutions were allowed to equilibrate over night after the phenanthrene and pyrene had been added. Solutions were subsampled (3 mL) and analyzed via fluorescence spectroscopy.

The PEDs were punctured with sixteen gauge stainless steel wire approximately every 3 cm in an accordion fashion. The wire was then bent into a circle with a 10 cm diameter and attached to a stainless steel rod, which could be rotated. Each PED was pulled so that it was flat against the wire in a circle. The first PED was spun at approximately 1 m/s in order to simulate the current that it would experience in the field. The second PED was not rotated in order to determine if the water boundary layer affected chemical uptake. When it had been confirmed that the solutions had come to equilibrium, the PEDs, approximately 1 gram in mass, were added to two of the beakers, and the PED in the first beaker was spun. The beakers were subsampled (3 mL) every 15 minutes initially and at longer time intervals after the first beaker had reached equilibrium (approximately

10 hours). The second beaker took much longer to reach equilibrium and was subsequently sampled twice a day, and then daily. The first experiment was conducted at 23°C. In order to measure the temperature dependence, the "spinning PED experiment" and the control were also performed at 5°C and 14°C.

The standard deviation for the equilibrium fluorescence intensities measured before the PEDs were added were on average within 4 and 5% of the mean for phenanthrene and pyrene, respectively. The standard deviations for the intensities measured once the PED and water had equilibrated were on average within 4 and 9% of the mean for phenanthrene and pyrene, respectively. The measured intensities were at the least 15 times greater intensities for only water.

A fourth experiment was performed at room temperature (22°C) with a PED of approximately half of the mass used for the three previous experiments. We were interested in determining if an increase in α would allow for a better fit with Equation (2.1); however, we did not observe any change in the data fit with the increased α. In this experiment the concentration of phenanthrene was 150 μg/L, which is 10 μg/L less than the concentration used in the first three experiments. The PED was extracted with hexane, and the phenanthrene and pyrene fluorescences were measured in this sample. Solutions of phenanthrene and pyrene in hexane of known concentration were made and used to create a calibration curve in order to calculate the concentration of each chemical present. The walls of the beakers were extracted with methylene chloride. Sodium sulfate was added to the extracts in order to remove any water that may have still been present. The samples were concentrated with a Kuderna Danish apparatus and transferred into a known

volume of hexane in order to measure the mass of phenanthrene and pyrene sorbed to the beaker walls. Solutions of phenanthrene and pyrene in water of known concentration were made in order to calculate the concentration of these chemicals present in the beakers at equilibrium.

Synchronous Fluorescence

Synchronous fluorescence allowed for the simultaneous measurement of the abundances of pyrene and phenanthrene. This method scans the emission and excitation spectra simultaneously with a constant wavelength interval, $\Delta\lambda$, between the emission and excitation wavelengths (Vo-Dinh, 1981). The measurements were made on a Perkin Elmer Luminescence Spectrometer LS 50B. The samples were scanned between 250 and 350 nm. An offset of 55 nm resulted in a distinct phenanthrene peak at 292 nm and two distinct pyrene peaks at 319 nm and 334.5 nm. The slit widths for the emission and excitation beams were set at 7 nm, and the scan speed was 1500 nm/min. Phenanthrene's intensity was measured at 292 nm and pyrene's intensity was measured at 319 nm. Fluorescence measurements were performed on the same sample five times in order to determine the instrument's precision. The measurement error (one standard deviation) for phenanthrene was measured to within 0.6% of the mean, while the measurement error (also one standard deviation) for pyrene measurements were within 1.3%.

RESULTS

Mass Balance

Fluorescence intensities for phenanthrene and pyrene were measured over time for our PED laboratory experiments performed at 23°C. A linear fit of the data, indicated that the fluorescence

intensities decreased by 6% for both phenanthrene and pyrene over the course of the experiment (130 hours; Figure 2.2). This result helps to exclude mechanisms other than uptake by the PED (e.g. biodegradation, volatilization, etc.) as the cause for the decrease in phenanthrene and pyrene fluorescence over time in the test beakers.

A mass balance was performed on the 22°C lab experiment (Table 2.1). For both phenanthrene and pyrene, the total mass measured was in good agreement with the mass added. For phenanthrene extracted from the beaker wall, an overlapping peak (d10-phenanthrene which had been added as a mass spectrometer recovery standard) prohibited us from measuring the intensity of phenanthrene. It can only be said that it was less that the height of the shoulder of the overlapping peak. However, the mass of phenanthrene and pyrene measured on the beaker walls of the experiment performed at 14°C was found to be 2 μg of phenanthrene for both the control beaker extract and the rotating PED beaker extract. If this is the value of phenanthrene on the wall the total phenanthrene recovered is 1471 μg, which is 98% of the mass added. For pyrene 99% of the chemical added was in the water or in the PED. These mass balances indicate that there was little or negligible photodegradation or biodegradation. Because 98% of phenanthrene and 99% of pyrene was found to be in one of two phases (water and PED), our assumption that this was a two-phase system appears to be a valid one.

Table 2.1. Masses of phenanthrene and pyrene measured in 22°C lab experiment at equilibrium.

Chemical	Mass in Water (μg)	Mass in PED (μg)	Mass on Wall (μg)	Total (μg)	Mass Added (μg)
Phenanthrene	998	471	<24	1469 - 1493	1500
Pyrene	56	142	3	201	200

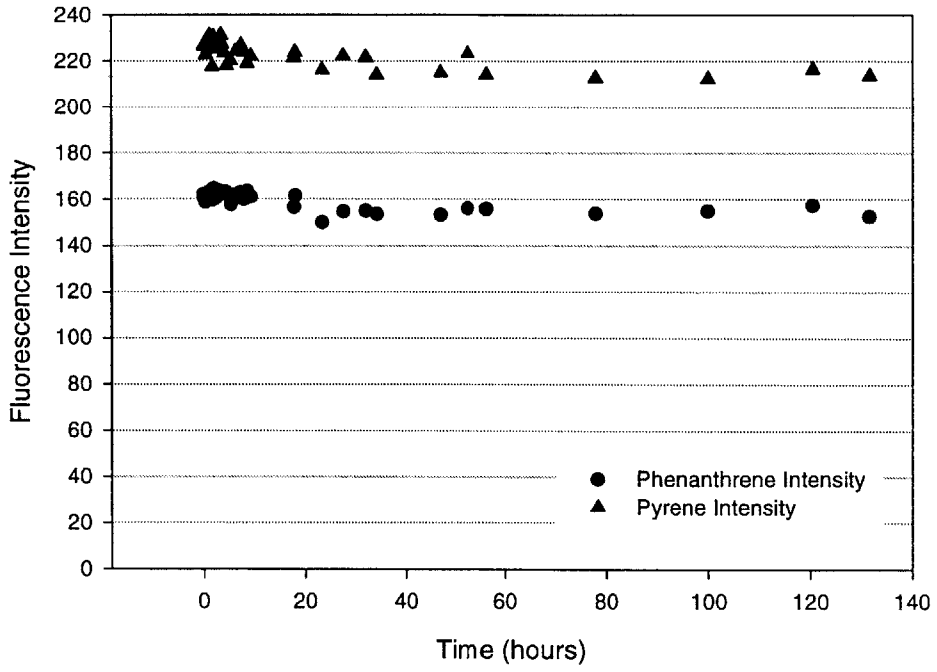

Figure 2.2. Fluorescence intensity vs. time for lab control @ 23°C.

Equilibrium Constants

Using Equation (2.9), initial and equilibrium intensities were used to calculate polyethylene-water partition coefficients (K_{PE}) for phenanthrene and pyrene (Table 2.2). The K_{PE} values measured at 22°C were significantly lower than the K_{PE} values measured at the other three temperatures. As discussed in the experimental section, approximately 0.5 grams of polyethylene were used in this experiment, while approximately 1 gram of polyethylene was used in the other three experiments. This was the only significant difference between the experiments. The cause for the divergent K_{PE} values measured during this experiment is not known.

To study the temperature dependence of K_{PE}, one must solve for K_{PE} as a function of temperature. By assuming that the aqueous activity coefficient was the only variable governing K_{PE} that had significant temperature dependence (i.e., $\Delta H_s^e \approx 0$), K_{PE} was related to the excess enthalpy of solution, ΔH_s^e (kJ/mol), in water.

$$\ln(K_{PE}) \cong \frac{\Delta H_s^e}{RT} + \text{constant} \qquad (2.18)$$

where R is the gas constant (kJ/molK), and T is the absolute temperature (K). The reader is referred to Schwarzenbach et al. (1993) for a more thorough discussion of this expression. A plot of *ln (K_{PE}) vs. 1/(RT)* for phenanthrene and pyrene was made in order to estimate ΔH_s^e (Figures 2.3 and 2.4). Using the method described, the $\Delta H_s^e \pm \sigma$ for phenanthrene was estimated to be 13 ± 9 kJ/mol and the $\Delta H_s^e \pm \sigma$ for pyrene to be 12 ± 10 kJ/mol; however, the R^2 values for these equation fits were poor: 0.50 for phenanthrene and 0.39 for pyrene. Schwarzenbach et al. (1993) estimate the ΔH_s^e for phenanthrene to be 18 kJ/mol; this value is within the error of this study's

estimate. The ΔH_s^e estimated for pyrene by Schwarzenbach et al. (1993) is 25 kJ/mol, which is outside the error of this study's estimate. When the anomalous K_{PE} value (22°C) was removed from the data set, and a plot of *ln* (K_{PE}) *vs. 1/(RT)* was made, $\Delta H_s^e \pm \sigma$ for phenanthrene was estimated to be 6 ± 3 kJ/mol and the $\Delta H_s^e \pm \sigma$ for pyrene to be 4 ± 3 kJ/mol. The R^2 values for these equation fits were 0.78 for phenanthrene and 0.69 for pyrene; however, these ΔH_s^e values are less similar to the ΔH_s^e values calculated including all four data sets.

The four laboratory-measured K_{PE} values were averaged (Table 2.3) and compared to values measured by other researchers. Huckins et al. (1993) measured $K_{PE,}$ for phenanthrene in polyethylene (Table 2.3). Huckins' value is within the error of this study's measured value for phenanthrene. The octanol-water partition coefficients (K_{OW}) for phenanthrene and pyrene increase with increasing molecular weight as did our polyethylene-water partition coefficients. The K_{PE} for pyrene was approximately five times that of the K_{PE} for phenanthrene, while the K_{OW} for pyrene is approximately four times that of phenanthrene.

Table 2.2. Polyethylene-water partition coefficients for phenanthrene and pyrene.

Experiment	Phenanthrene $(mol/L_{PE})/(mol/L_W)$	Pyrene $(mol/L_{PE})/(mol/L_W)$
Temperature @ 23°C	16,000 ± 1000	95,000 ± 7000
Temperature @ 22°C	12,000 ± 1000	63,000 ± 3000
Temperature @ 14°C	19,000 ± 2000	94,000 ± 17,000
Temperature @ 5°C	19,000 ± 2000	100,000 ± 20,000

Table 2.3. Polyethylene-water and octanol-water partition coefficients for phenanthrene and pyrene.

Chemical	Average K_{PE} (This Study) $(mol/L_{PE})/(mol/L_W)$	K_{PE} (Huckins et al., 1993) @ 18°C $(mol/L_{PE})/(mol/L_W)$	K_{OW} (Schwarzenbach et al., 1993) $(mol/L_{PE})/(mol/L_W)$
Phenanthrene	17,000 ± 1000	16,000	37,000
Pyrene	89,000 ± 6000	---	135,000

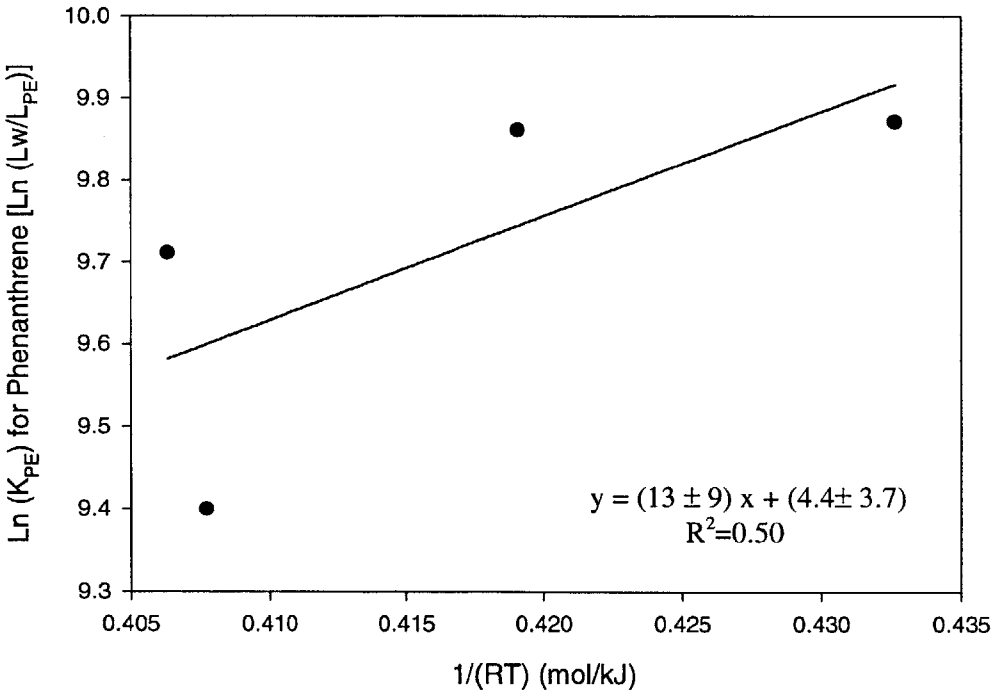

Figure 2.3. Natural log of K_{PE} for phenanthrene vs. 1/(RT).

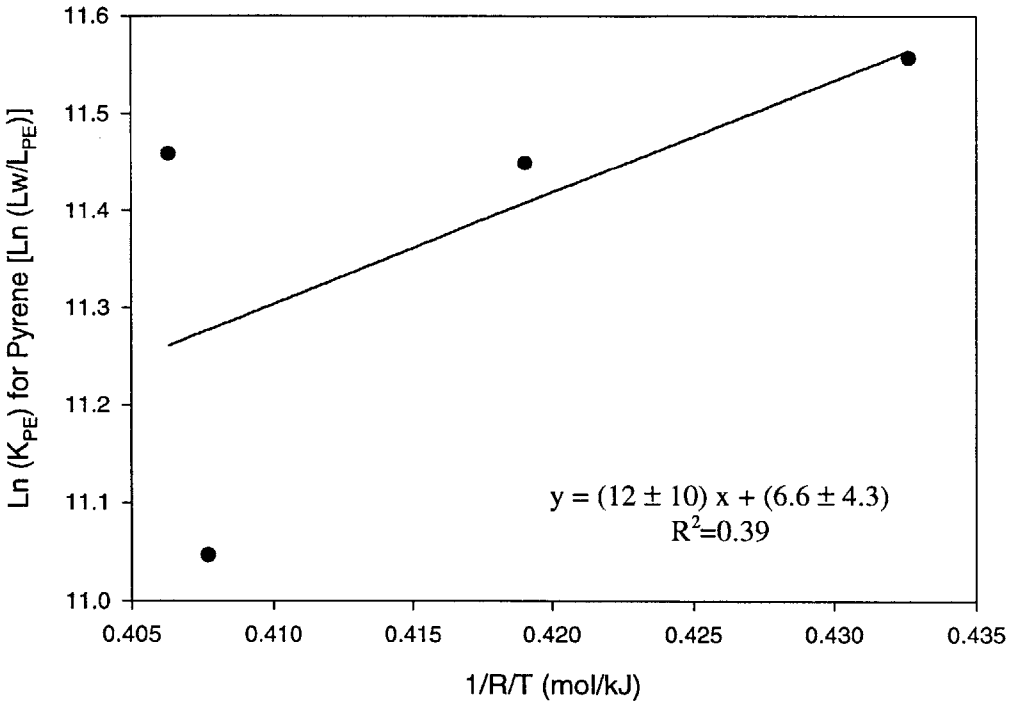

Figure 2.4. Natural log of K_{PE} for pyrene vs. 1/(RT).

Diffusivity

In order to estimate the concentration of HOCs extracted from PEDs that have not equilibrated with the surrounding water, each chemical's diffusivity in polyethylene is needed. Diffusivities can be measured in the laboratory and used to solve for the dissolved concentration of each chemical in the field. The intensity data collected during the lab experiments were fit to Equation (2.1). A best fit was used to solve for the diffusivity of each chemical in polyethylene at 23°C (Figures 2.5 and 2.6). Equation (2.1) appears to fit the phenanthrene data quite well, but does not fit the pyrene data nearly as well. For pyrene, diffusion is slower than the fitted value initially and then becomes greater than the calculated diffusivity after the first two hours. This trend is also visible for phenanthrene, but to a lesser extent. The best fits for the experiments at 5°, 14°, and 22°C show the same results as the experiment at 23°C (Tables 2.4 and 2.5). The intensity data for the laboratory experiments suggested that the diffusivity of pyrene was increasing with time. The same was true for phenanthrene, but to a lesser extent.

Table 2.4. Phenanthrene diffusivities in polyethylene from best fit with Equation (2.1).

Phenanthrene Experiment	Diffusivity from Eqn. 2.1 (cm^2/s)		Time-Dependent Diffusivities (cm^2/s)	Average of Time-Dependent Diffusivities
Temp. @ 5°C	7.5E-11	D_1	3.9E-11	1.3E-10
		D_2	1.4E-10	
		D_3	2.1E-10	
Temp. @ 14°C	9.70E-11	D_1	5.90E-11	1.2E-10
		D_2	1.90E-10	
		D_3	1.00E-10	
Temp. @ 22°C	2.30E-10	D_1	1.50E-10	2.1E-10
		D_2	3.70E-10	
		D_3	1.10E-10	
Temp. @ 23°C	2.30E-10	D_1	1.40E-10	2.7E-10
		D_2	5.90E-10	
		D_3	8.40E-11	

Table 2.5. Pyrene diffusivities in polyethylene from best fit with Equation (2.1).

Pyrene Experiment	Diffusivity from Eqn. 2.1 (cm^2/s)		Time-Dependent Diffusivities (cm^2/s)	Average of Time-Dependent Diffusivities
Temp. @ 5°C	8.5E-12	D_1	2.8E-12	2.4E-11
		D_2	1.5E-11	
		D_3	5.5E-11	
Temp. @ 14°C	1.00E-11	D_1	4.40E-12	2.1E-11
		D_2	2.00E-11	
		D_3	3.90E-11	
Temp. @ 22°C	2.40E-11	D_1	7.80E-12	4.8E-11
		D_2	3.50E-11	
		D_3	1.00E-10	
Temp. @ 23°C	2.70E-11	D_1	9.40E-12	7.5E-11
		D_2	8.60E-11	
		D_3	1.30E-10	

Time-Dependent Diffusivity

The hypothesis that diffusivity is a function of time was investigated by performing a best-fit using Equations (2.16) and (2.17) for the 23°C experiment. The diffusivities over three time intervals were calculated in order to evaluate the hypothesis that diffusivity was increasing with time. The times for the steps were chosen arbitrarily. Phenanthrene diffusivities increased with time over the first two time intervals; however, the diffusivity for the final time interval was less than the first two (Figure 2.7). The increasing diffusivity over time was most apparent for pyrene (Figure 2.8). Diffusivity increased from 9.4E-12 cm^2/s to 8.6 E-11 cm^2/s to 1.3E-10 cm^2/s with each successive time interval. The same trend was observed for the best-fit pyrene diffusivities for the 5°, 14°, and 22°C lab experiments (Tables 2.4 and 2.5)

The data was also fit to the model allowing for two diffusivities. The time for the interval end points was chosen arbitrarily. As expected, the time-dependent/two-diffusivity model fit the phenanthrene data well (Figure 2.9). The pyrene model fit quite well (Figure 2.10); however, because the diffusivity increased by an order of magnitude, there is a noticeable discontinuity between time intervals. It is important to note that the choice of different time intervals may result in different trends in diffusivity with respect to time. This was not explored in this study.

There are several causes for the time-dependence of diffusivity. Several researchers have found diffusivity to be a function of the concentration of the solute (Doong and Ho, 1993; Rogers et al., 1960; Barrer and Fergusson, 1957). In fact, this dependence has been seen at volume fractions as low as 1% (Doong and Ho, 1993; Barrer and Fergusson, 1957); however, our volume fractions are 0.1% for phenanthrene and 0.03% for pyrene. A concentration-dependent form of Fick's law cannot describe the diffusion behavior of many polymers; these polymers are said to exhibit non-Fickian behavior. In rubbery or amorphous polymers, diffusion is generally Fickian; however, in glassy or crystalline polymers, the diffusion is often non-Fickian. Polymers in the rubbery state respond quickly to changes in their condition, while glassy polymers have time-dependent properties. As our polyethylene is semicrystalline, non-Fickian diffusivity may result in the observed time dependence. A third possibility is that diffusivity is a function of distance. For example, if the outer portion of the membrane differs from the inside portion, these heterogeneous properties may result in the observed increase in diffusivity over time.

Several researchers have measured the diffusivities of hydrocarbons in polyethylene (Doong and Ho, 1992; Aminabhavi and Naik, 1998; Flynn, 1982). However, only one value for the diffusivity

of phenanthrene in polyethylene and one for the diffusivity of pyrene in polyethylene were found in the literature (Huckins et al., 1993; Simko et al., 1999). An attempt was made to correlate hydrocarbon diffusivity with molecular weight and molar volume. However, these correlations did not allow for reasonable estimates of higher molecular weight PAHs (phenanthrene and pyrene). Several models for the estimation of diffusivity in polyethylene and other polymers have been proposed (Fujita, 1960; Vrentas and Duda, 1977; Pace and Datyner, 1979; Salame, 1986; Doong and Ho, 1992). Unfortunately, the use of one of these models to estimate diffusion coefficients resulted in estimates differing from the measured values by several orders of magnitude (Salame, 1986). The others required several parameters that were difficult to find in the literature for our chemicals or would have to be solved for with diffusivity data sets (Fujita, 1960; Vrentas and Duda, 1977; Pace and Datyner, 1979; Doong and Ho, 1992). Huckins et al. (1983) measured a diffusion coefficient for phenanthrene in SPMDs (Table 2.6). Although, the diffusivity measured by Huckins et al. is for diffusion through triolein and polyethylene, one might expect the diffusion through a plastic to be much slower than that through a liquid and, would, consequently, expect this diffusivity to be similar to the diffusivity in polyethylene alone. These phenanthrene diffusivity values were within a factor of three of each other.

Simko et al. (1999) measured the diffusivity of pyrene in low-density polyethylene to be 5E-10 cm^2/s; this is more than an order of magnitude greater than this study's measured value of 3E-11 cm^2/s. It is important to note, however, that the experimental set up of Simko et al. was very different from the one used here. They measured the concentrations of pyrene in a polyethylene sheet composed of five layers. In order to prepare this five-layer sheet, they heated and pressed the

polyethylene for several minutes. This heating and cooling may have a significant effect on the crystallinity of the polymer, which may have affected the diffusivity (Barrer, 1968).

Table 2.6. Diffusivities in polyethylene measured for phenanthrene and pyrene.

Chemical	This Study (cm^2/s @ 23°C)	Huckins et al., 1993 (cm^2/s @ 18°C)	Simko et al., 1999 (cm^2/s @ 24°C)
Phenanthrene	2E-10	≥ 7E-11	
Pyrene	3E-11		5E-10

Temperature-Dependent Diffusivity

In order to adjust diffusivity for temperature, it is necessary to know the diffusivity activation energy. The Arrhenius equation can be used to solve for this energy.

$$D = A\exp(-E/RT) \qquad (2.19)$$

where A is a pre-exponential factor (cm^2/s) and E is the activation energy (kJ/mol). A plot of $ln(D)$ vs. $1/(RT)$ allowed the use of the slope to solve for the activation energy of diffusion for phenanthrene and pyrene (Figures 2.11 and 2.12). The diffusivity estimated from Equation (2.1) was used. With this method, the activation energy ± one standard deviation for phenanthrene (46 ± 10 kJ/mol) and pyrene (45 ± 12 kJ/mol) were estimated. The data fit the equation with R^2 values of 0.91 for phenanthrene and 0.88 for pyrene. Activation energies for the diffusivity of about 40 different hydrocarbons in low-density polyethylene compiled by Flynn (1982) ranged from 34 to 87 kJ/mol. These estimated activation energies are within this range.

Diffusivity as a Function of Molar Volume

The diffusivity of chemicals in water has been observed to relate to the molar volume of the chemical (Schwarzenbach et al., 1993). Such a correlation for chemical diffusivity in low-density polyethylene may be useful because the molar volume for chemicals is more readily available in the literature and is easier to estimate than the diffusivity of chemicals, specifically PAHs in low-density polyethylene. We correlated the diffusivities of benzene, phenanthrene, and pyrene with the molar volume for these chemicals (Figure 2.13). Three different measurements for the diffusivity for benzene in low-density polyethylene were used in the graph (Flynn, 1982). These diffusivities were for benzene concentrations approaching zero which are the levels of concentration in these experiments. The diffusivities were adjusted to 23°C. Characteristic molar volumes were calculated according to Abraham and McGowan (1987). This is not a robust data set, and this correlation is tentative. As this correlation was based on only five measurements, more diffusivity measurements for PAHs in polyethylene are needed.

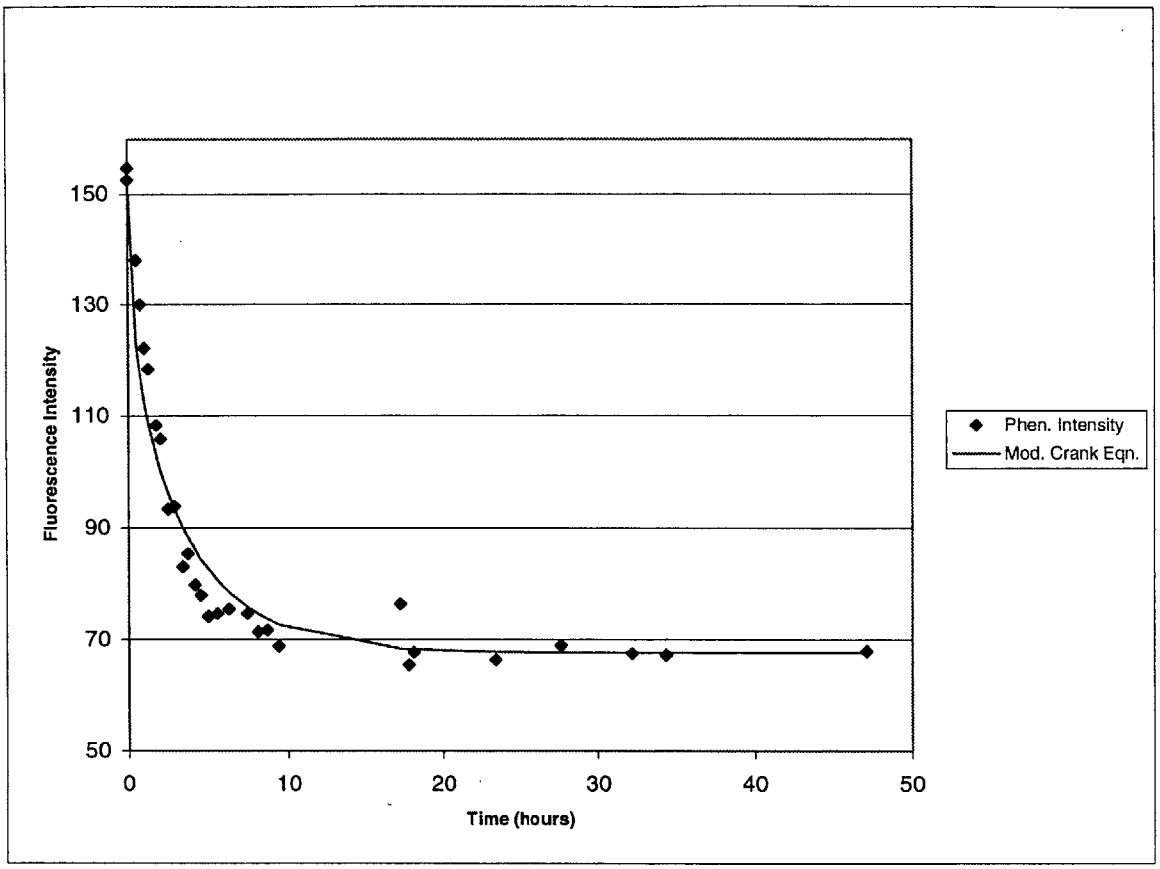

Figure 2.5. Phenanthrene intensity vs. time; PED at 23°C; α=0.691; D=2.3x10^{-10} cm^2/s.

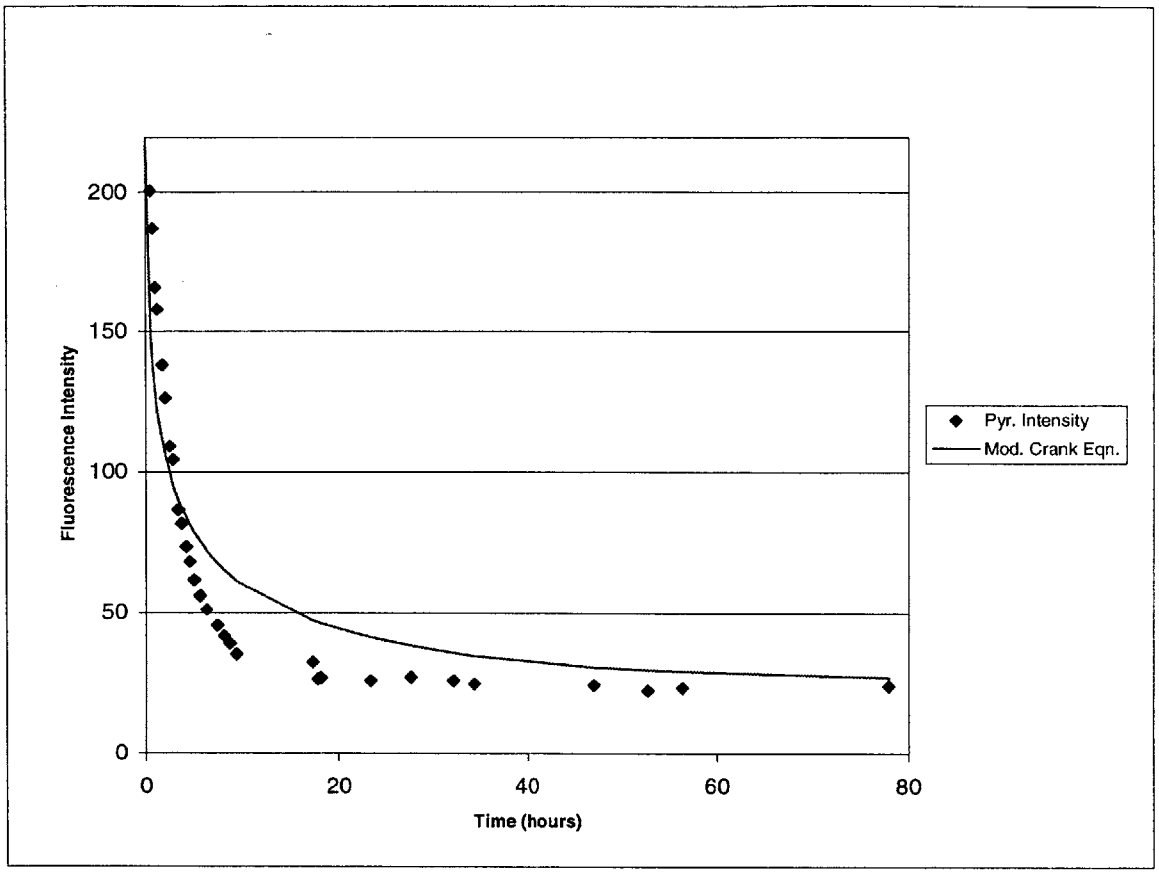

Figure 2.6. Pyrene intensity vs. time; PED at 23°C; α=0.130; D=2.7×10^{-11} cm^2/s.

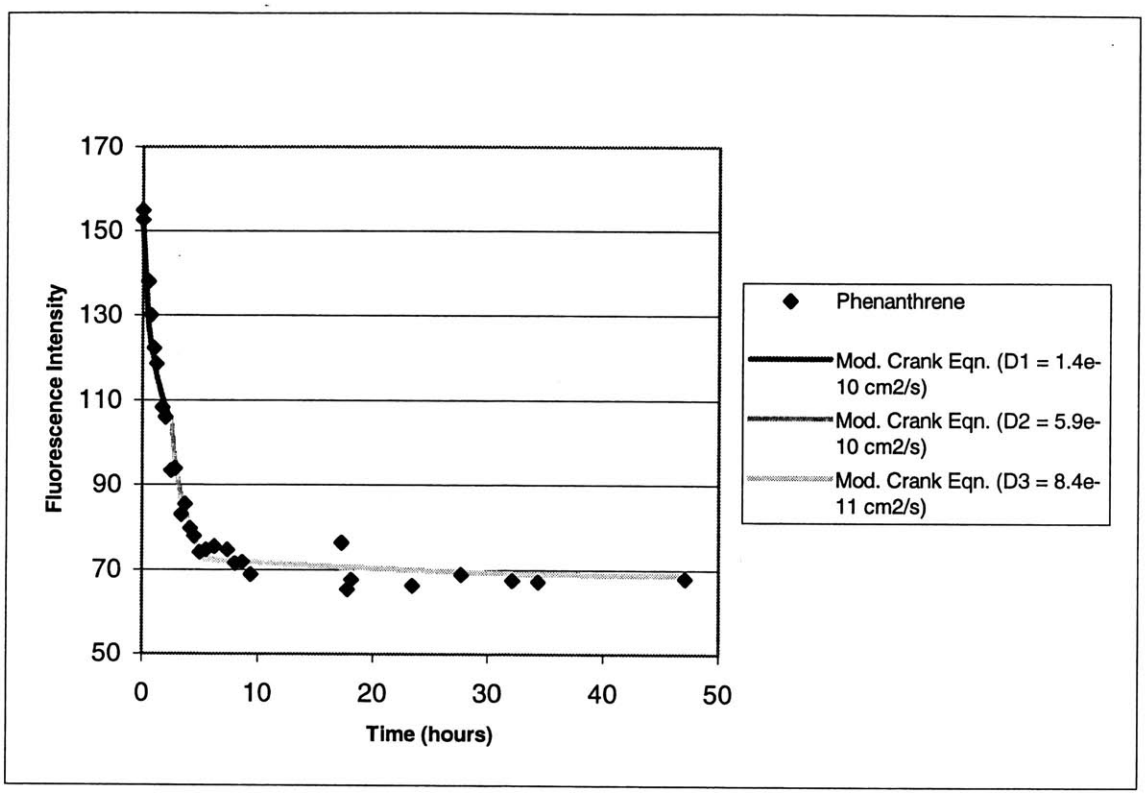

Figure 2.7. Phenanthrene intensity vs. time; PED at 23°C; α=0.691; time-dependent diffusivity.

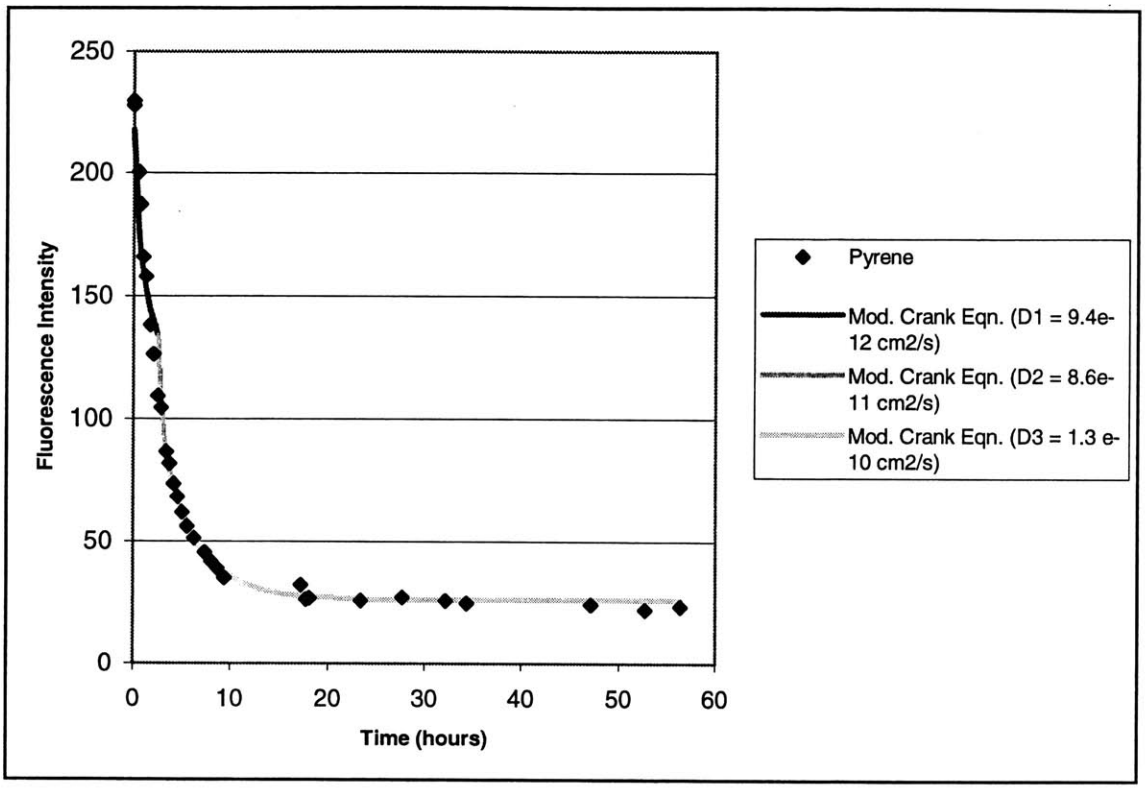

Figure 2.8. Pyrene intensity vs. time; PED at 23°C; α=0.130; time-dependent diffusivity.

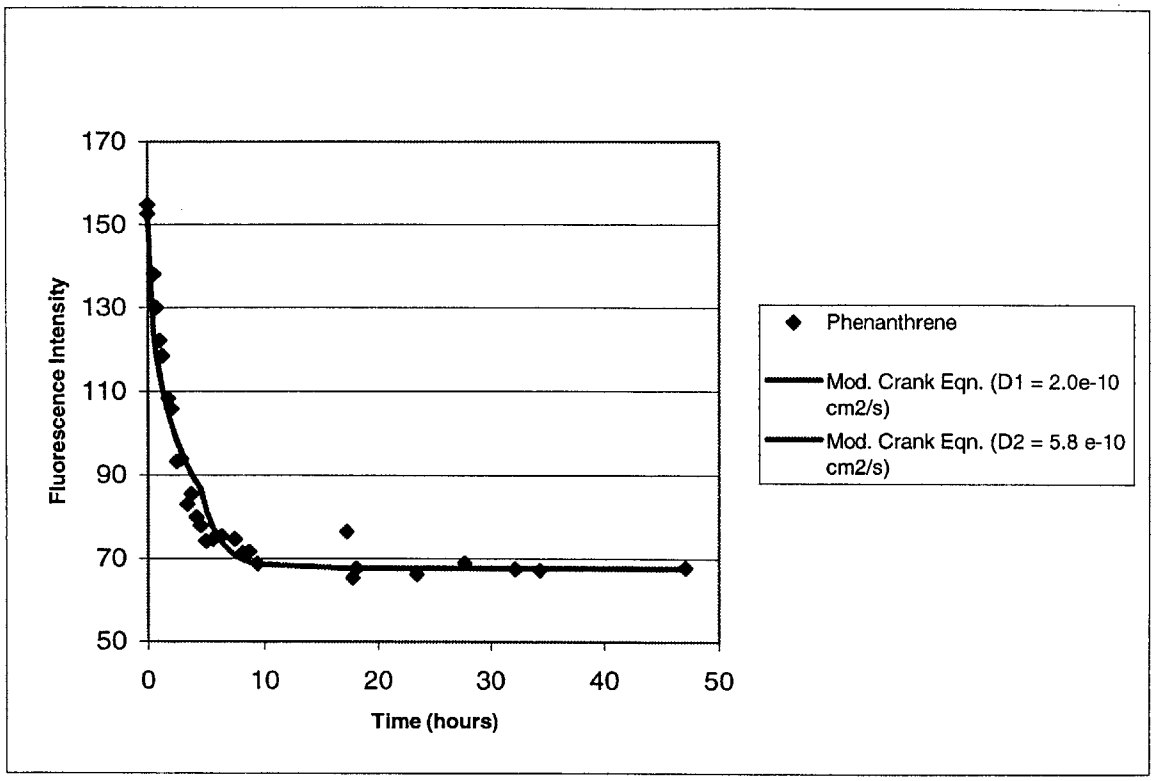

Figure 2.9. Phenanthrene intensity vs. time; PED at 23°C; α=0.691; time-dependent diffusivity.

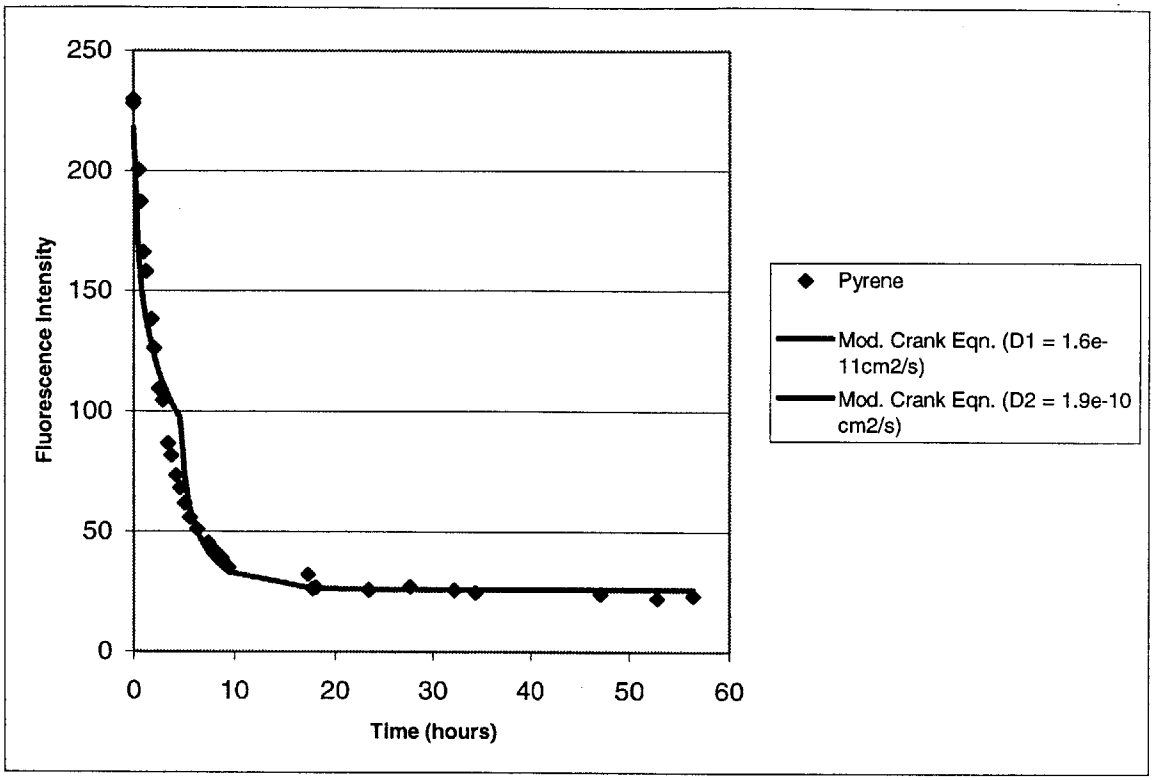

Figure 2.10. Pyrene intensity vs. time; PED at 23°C; α=0.130; time-dependent diffusivity.

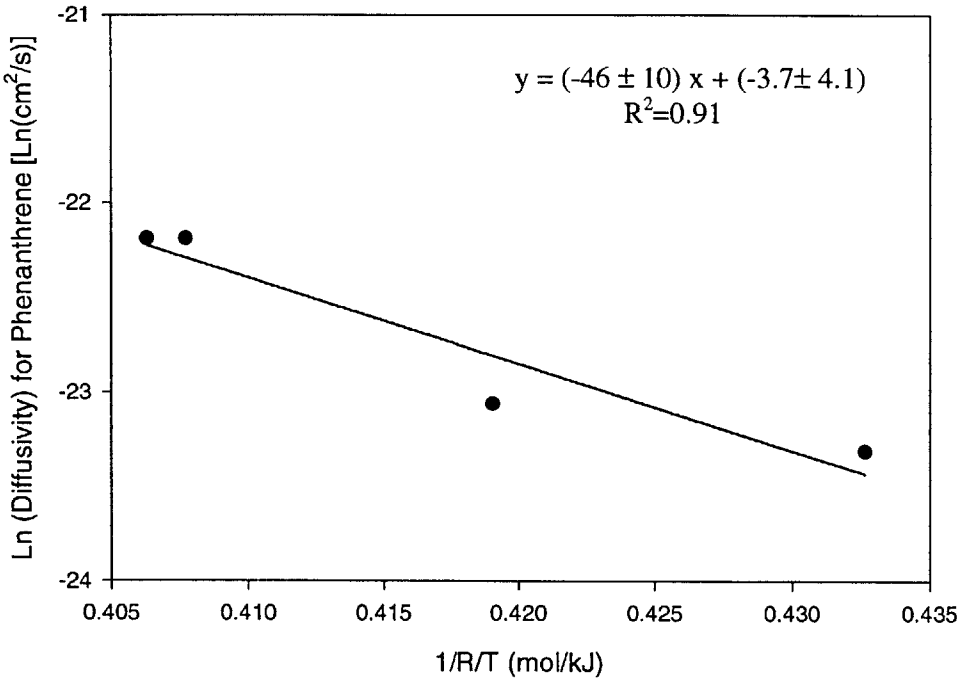

Figure 2.11. Natural log of diffusivity for phenanthrene vs. 1/(RT).

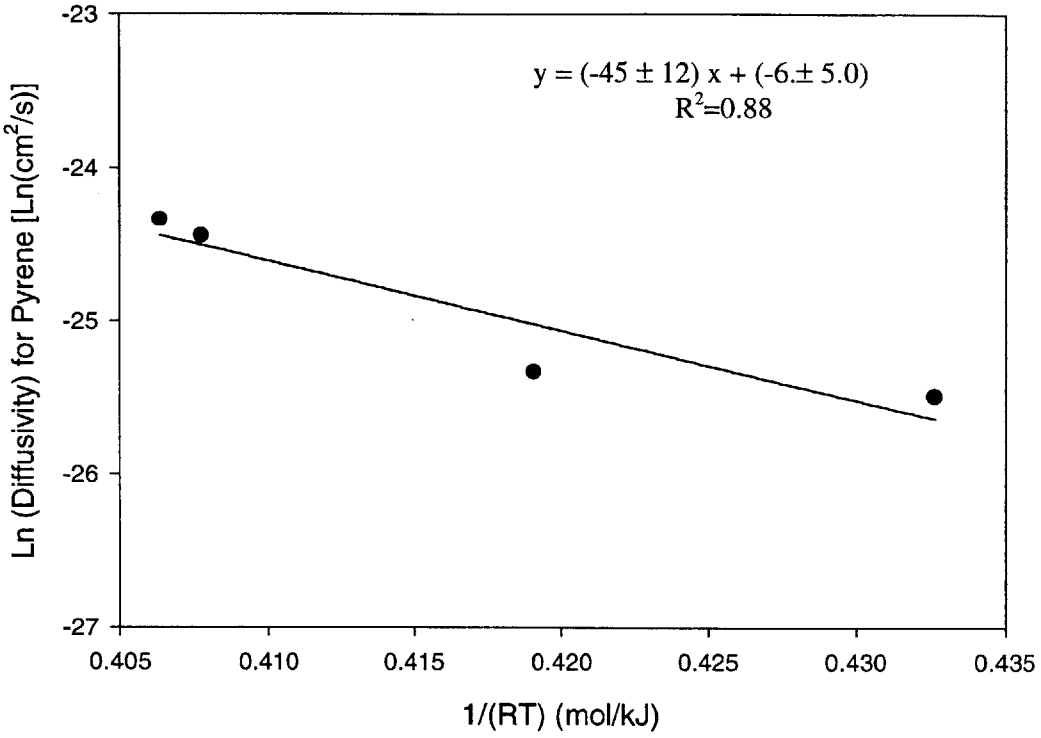

Figure 2.12. Natural log of diffusivity for pyrene vs. 1/(RT).

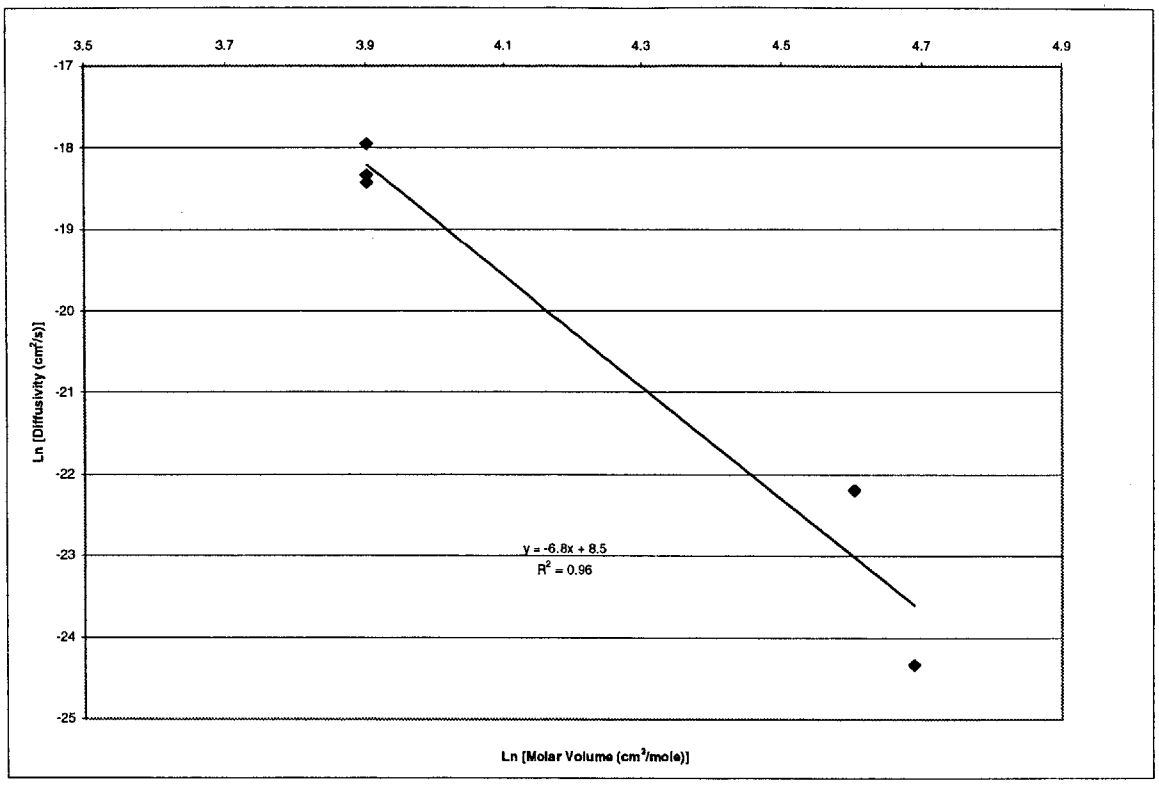

Figure 2.13. Natural log of diffusivity vs. natural log of molar volume.

Time for 95% Equilibrium

Based on the diffusivities calculated with Equation (2.1), the time for phenanthrene and pyrene to reach 95% of equilibrium in an infinite bath was estimated with Equation (2.7) (Table 2.7).

Table 2.7. Time for 95% of equilibrium (days) in an infinite bath.

Experiment	**Phenanthrene** (days)	**Pyrene** (days)
Exp. @ 23°C	0.9	7
Exp. @ 22°C	0.9	8
Exp. @ 14°C	2	20
Exp. @ 5°C	3	20

Clearly, temperature plays an important role in the rate of uptake. For this reason, it is important to adjust diffusivity with the activation energy to the temperature of the water being sampled before calculating the C_w. It may be helpful to estimate this time before sampling in the field in order to plan the time for PED deployment.

The Effects of Current on Uptake Rate

Looking at the intensity vs. time data for phenanthrene and pyrene in the laboratory experiments performed at 23°C, one notices a significant difference in the time for equilibrium between the rotating PED and the stationary PED (Figures 2.14 and 2.15, respectively). The intensity of phenanthrene in the solution with the PED spinning at approximately 1 m/s approached equilibrium after 5 hours, while the intensity for phenanthrene in solution with the stationary PED had not reached equilibrium even after 130 hours. The pyrene intensity in the solution with the

spinning PED approached equilibrium after 10 hours. For the stationary PED, the pyrene had not yet reached equilibrium after 130 hours.

The PED's motion in the water appears to have a significant effect on the uptake rate of the chemical. This may be due to a reduction in the water boundary layer allowing for an increase in uptake rate. This spinning may also allow more "packets" of water to come into contact with the PED than do in the case for the non-spinning PED. This result indicates the importance of performing laboratory experiments that will match the field conditions as closely as possible.

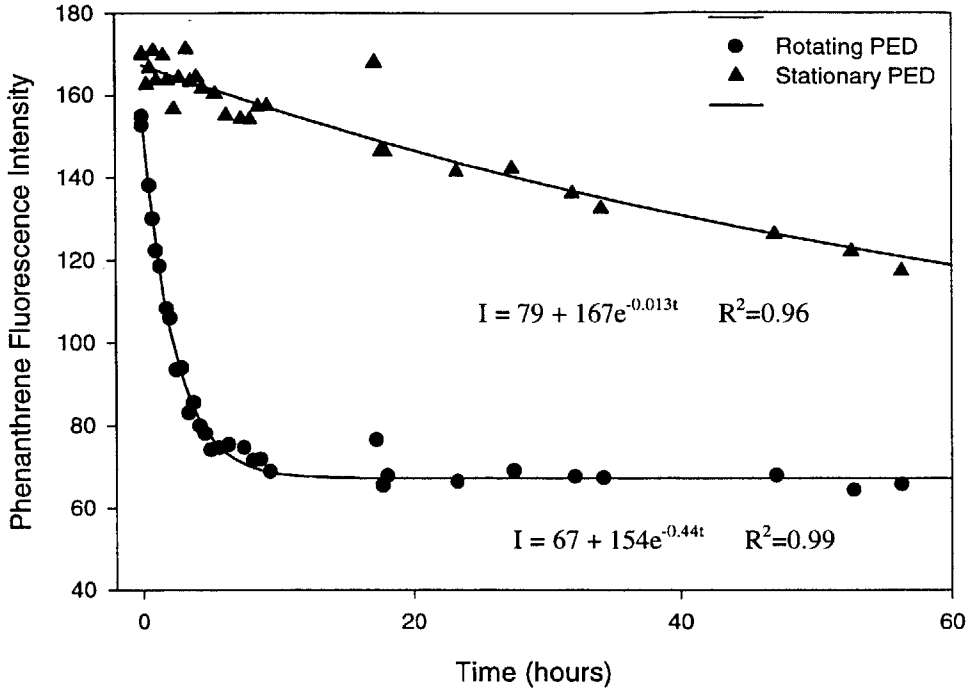

Figure 2.14. Fluorescence intensity vs. time for phenanthrene @ 23°C.

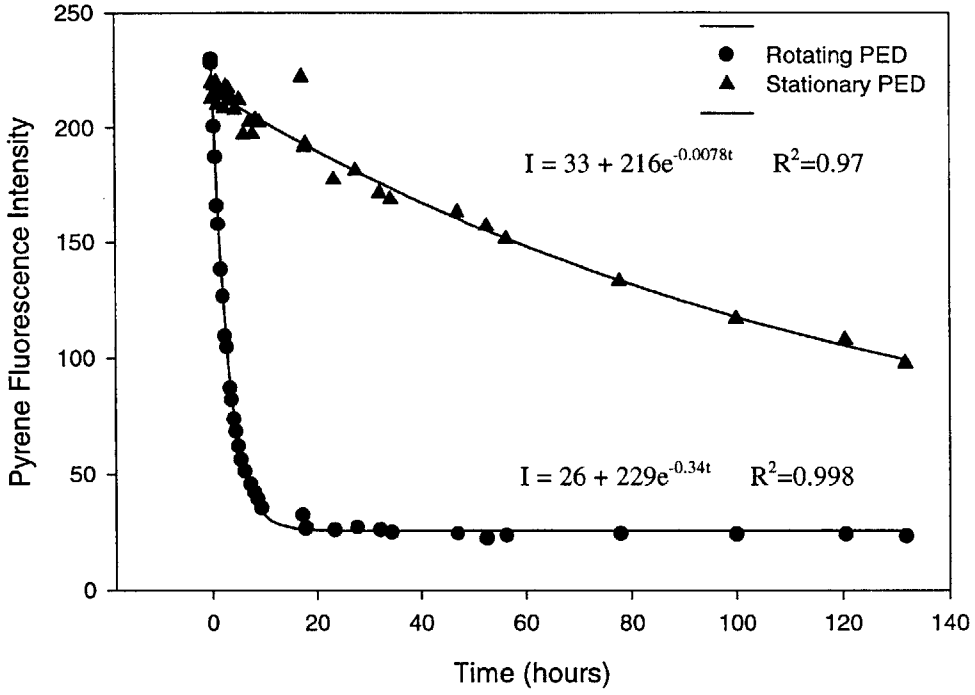

Figure 2.15. Fluorescence intensity vs. time for pyrene @ 23°C.

Exponential Decay

Because our fluorescence intensity vs. time data for both phenanthrene and pyrene appeared to follow an exponential decay model, they were fit to such a model.

$$I_w = I_{eq} + (I_{w0} - I_{eq})e^{-kt} \qquad (2.20)$$

where I_w, I_{eq}, and I_{wo}, are the fluorescence intensities in the water at time t, equilibrium, and initially, respectively. k is the time constant for PED uptake. Sigma Plot was used to fit the data to Equation (2.20) (Figures 2.14 and 2.15). When the PED was spinning, the uptake rate, k, was much larger than for the non-spinning case. In the spinning PED experiment, $k = 0.44$ hr^{-1} for phenanthrene, and $k = 0.34$ hr^{-1}. When the PED was stationary, the uptake rate was much slower: $k = 0.013$ hr^{-1} for phenanthrene and 0.0078 hr^{-1} for pyrene. For all four data fits, the R^2 value was 0.96 or greater. This observation is difficult to explain. The results are consistent with a film model and appear to fit this type of model quite well. However, the system was not at steady state.

APPLICATIONS

Initial experiments indicate that PEDs are a useful device for the measurement of dissolved polycyclic aromatic hydrocarbons in the water column. Polyethylene is readily available and inexpensive. Polyethylene devices will prove to be useful under many circumstances.

(1) PEDs allow for the measurements of hydrophobic organic contaminants (e.g., PAHs) that are "truly dissolved". "Truly dissolved" refers to those chemicals which are not sorbed to particulate matter or colloids. This truly dissolved fraction is the fraction that is most readily bioavailable. If the chemical is toxic or carcinogenic, this dissolved fraction may be harmful to the

surrounding organisms. The chemical signals measured in the PEDs may also provide insight into the sources of this bioavailable fraction.

(2) As PEDs require days (depending on the chemical and temperature) to reach equilibrium with the surrounding water, they allow for a time-averaged measurement. This is useful for determining the level of pollutant exposure for organisms living in the sampled environment. Using different PED thicknesses will allow for the measurement of varying lengths of time.

(3) The large polyethylene-water partition coefficients for PAHs make the measurement of small concentrations of PAHs much less labor intensive than the extraction of large volumes of water. These large partition coefficients will facilitate the extraction of a mass of chemical that is greater than the analyzer's detection limit. Generally, these larger concentrations will allow for more accurate measurements.

REFERENCES

Abraham, M. H., J. C. McGowan. 1987. The use of characteristic volumes to measure cavity terms in reversed phase liquid chromatography. *Chromatographia* **23**, 243-246.

Aminabhavi, T. M. and H. G. Naik. 1998. Chemical compatibility study of geomembranes—sorption/desorption, diffusion and swelling phenomena. *J. Haz. Mat.* **60**, 175-203.

Barrer, R. M. 1968. Diffusion and permeation in heterogeneous media. In *Diffusion in Polymers,* Crank, J. and G. S. Park (Eds.), Academic Press, London. pp. 165-217.

Barrer, R. M. and R. R. Fergusson. 1958. Diffusion of benzene in rubber and polyethene. *Trans. Faraday Soc.* **54**, 989-1000.

Carson, R. 1962. *Silent Spring*; Houghton Mifflin, Boston. 368 pp.

Crank, J. 1975. *The Mathematics of Diffusion*, 2nd ed.; Oxford University Press, London. 414 pp.

Doong, S. J. and W. S. Winston Ho. 1992. Diffusion of hydrocarbons in polyethylene. *Ind. Eng. Chem. Res.* **31**, 1050-1060.

Farrington, J. W.; E. D. Goldberg, R. W. Risebrough, J. H. Martin, and V. T. Bowen. 1983. U.S. "Mussel Watch" 1976-1978: An overview of the trace-metal, DDE, PCB, hydrocarbons, and artificial radionuclide data. *Env. Sci. Technol.* **17**, 490-496.

Flynn, J. H. 1982. A collection of kinetic data for the diffusion of organic compounds in polyolefins. *Polymer* **23**, 1325-1344.

Fujita, K., A. Kishimoto, K. Matsumoto. 1960. Concentration and temperature dependence of diffusion coefficients for systems polymethyl acrylate and n-alkyl acetates. *Trans. Faraday Soc.* **56**, 424.

Huckins, J. N., G. K. Manuweera, J. D. Petty, D. Mackay, and J. A. Lebo. 1993. Lipid-containing semipermeable membrane devices for monitoring organic contaminants in water. *Env. Sci. Technol.* **27**, 2488-2496.

McElroy, A. E., J. W. Farrington, and J. M Teal. 1990. Influence of mode of exposure and the presence of a tubiculous polychaete on the fate of benz(a)anthracene in the benthos. *Env. Sci. Technol.* **24**, 1648-1655.

Miller, R. L. 1965. Crystalline and Spherulitic Properties In *Crystalline Olefin Polymers Part I*, R. A. V. Raff and K. W. Doak (Eds.), John Wiley and Sons Inc., New York. pp. 577-676.
Pace, R. J. and A. Datyner. 1979. Statistical mechanical model of diffusion of complex penetrants in polymers. II. applications. *J. Poly. Sci.: Poly. Phys. Ed.* **17**, 1693-1708.

Rogers, C. E., V. Stannett, and M. Szwarc. 1960. The sorption, diffusion, and permeation of organic vapors in polyethylene. *J. Poly. Sci.* **45**, 61-82.

Salame, M. 1986. Prediction of gas barrier properties of high polymers *Polymer Eng. Sci.* **26**, 1543-1546.

Schwarzenbach, R. P., P. M. Gschwend, and D. M. Imboden. 1993. *Environmental Organic Chemistry*; John Wiley and Sons, Inc., New York. 681 pp.

Simko, P, P. Simon, V. Khunova. 1999. Removal of polycyclic aromatic hydrocarbons from water by migration into polyethylene. *Food. Chem.* **64**, 157-161.

Simond, H. R. and J. M. Church. 1963. *A Concise Guide to Plastics*, 2nd ed.: Reinhold Publishing Corporation, New York. 392 pp.

Vo-Dinh, T., Synchronous Excitation Spectroscopy. 1981. In *Modern Fluorescence Spectroscopy*, E. L. Wehry (Ed.), Plenum Press, New York. pp.167-192.

Vrentas, J. S. and J. L Duda. 1977. Diffusion in polymers-solvent systems: II. A predictive theory for the dependence of diffusion coefficients on temperature, concentration, and molecular weight. *J. Polym. Sci., Polym. Phys. Ed.* **15**, 417.

Whitman, W. G. 1923. The two-film theory for gas absorption. *Chem. Metal. Eng.* **29**, 146-148.

CHAPTER 3: SEDIMENT-WATER EXCHANGE OF POLYCYCLIC AROMATIC HYDROCARBONS IN THE LOWER HUDSON ESTUARY

INTRODUCTION

Once in the aquatic environment, hydrophobic organic contaminants (e.g., polycyclic aromatic hydrocarbons; PAHs) preferentially associate with the sediments. Consequently, even after the input of these contaminants is reduced or eliminated, the sediments may still serve as a large source of pollutants to the water column. Recent studies indicate that the sediments of urban water bodies (e.g., lower Hudson Estuary, Boston Inner Harbor) are a source of hydrophobic organic contaminants to the overlying water (Achman et al., 1996; Flores, 1998; Petroni and Israelsson, 1998; Mitra et al., 1999). In more sheltered and quiescent harbors, the transfer of pollutants from the sediments to the water column is likely due to diffusive fluxes (e.g., Boston Harbor), while in areas with episodic resuspension events (e.g., the lower Hudson Estuary) one would expect these particle resuspensions to result in greater fluxes of contaminants to the water column. Estuaries often have higher levels of suspended solids than either the river supplying them with the sediment or the adjacent ocean. These elevated particle concentrations are the result of sediment trapping. We studied the lower Hudson Estuary in order to examine the effects of sediment resuspension on the concentrations of PAHs in the water column.

Because of elevated concentrations of PAHs and polychlorinated biphenyls (PCBs) in sediments, parts of the lower Hudson Estuary are considered to be areas of environmental concern (Wolfe et al., 1996). The dissolved fraction of PAHs is more readily bioavailable than the particle-sorbed fraction (Neff, 1979; McElroy et al., 1990) and is therefore of great interest. However, once the dissolved fraction is taken up by organisms, more of the sorbed fraction may dissolve. For this

reason, it is important to determine the total (sorbed and dissolved) PAHs present as well as the physiochemical parameters that may influence the distribution of PAHs so that the transport of these chemicals within the environment can be better understood. While it is the dissolved fraction that directly effects the organisms present, it is important to measure the total PAH pool as well as the dissolved fraction.

In addition to quantifying the dissolved fraction, it is useful to determine the source of this fraction. Farrington et al. (1983) have hypothesized that petroleum hydrocarbons are available for biological uptake to a greater extent than pyrogenic source hydrocarbons. Petroleum inputs would most likely be dissolved, colloidal, or associated with particles. In contrast, pyrogenic compounds are more likely to be strongly sorbed to, or incorporated into, particles from pyrogenic sources. Examining the chemical signals of PAH samples may allow us to determine the sources of the dissolved and sorbed fractions.

The objective of this chapter is to better understand the effects of sediment resuspension on the input of PAHs to the water column and the sources for these chemicals. Studying the distributions of PAHs in the lower Hudson River estuary in conjunction with the physicochemical environmental parameters will provide for a better understanding of the mechanisms governing the fate of these chemicals in the environment.

SITE DESCRIPTION

The lower Hudson River Estuary empties into New York Harbor and is bordered by northern New Jersey to the west and Manhattan Island and New York City to the east. Samples were taken along

the lower Hudson River Estuary between New York Harbor and the town of Hastings about 34 km up river (Figure 3.1). There were three primary sampling sites: the Southern Site at the Battery which is located next to the southern tip of Manhattan where the Hudson empties into New York Harbor, the Estuarine Turbidity Maximum (ETM) approximately 13 km up the river, and the Northern Site which is approximately 34 km up the river from the Battery near the town of Hastings. The Northern Site was chosen to allow for the estimation of the input of PAHs flowing into the estuary. As the ETM was observed to be the area of maximum resuspension, it would allow for the estimation of the sources of PAHs from sediment resuspension. The Battery was chosen to represent the output of PAHs from the estuary.

The lower Hudson River estuary has been observed to have two estuarine turbidity maxima on the western side of the river (Figure 3.1; Hirshberg and Bokuniewicz, 1991). Geyer (1995) observed near bottom suspended solids concentrations between 100 and 200 mg/L in the summer of 1992 and between 100 and 400 mg/L concentrations during high discharge in 1993 at the southern estuarine turbidity maximum site where we sampled (Figure 3.1). However, these elevated suspended solid concentrations were observed to drop to nearly zero at slack tide, indicating the tidal influence of sediment resuspension. Tidal cycles also influence suspended solid concentrations. During spring tides, which are tides of greater-than-average change in water level around the times of new and full moon, near-bottom suspended sediment concentrations were found to reach values as high as 1800 mg/L. In contrast, near-bottom, suspended sediment levels during neap tide, which is a tide of minimum change in water level occurring during the first and third quarters of the moon, were approximately six times less (Figure 3.2; Geyer et al., 1999).

The distance of salt-water intrusion up the Hudson from the Battery varies from ~30 km during high freshwater discharge in the spring to ~100 km during low discharge in the fall (Abood, 1978). The net flow in the Hudson Estuary is dominated by tidal flow even during times of high discharge; tidal flow is between 10 and 100 times greater than freshwater flow (Cooper et al., 1988). Geyer (1995) observed maximum flood currents to be ~0.8 m/s and maximum ebb currents to be 1.2 m/s during low discharge conditions in 1992. During high discharge conditions, Geyer (1995) observed maximum flood and ebb currents to be 1.5 m/s. However, there does not appear to be a correlation between current velocity and suspended load (Figure 3.2; Geyer et al., 1999).

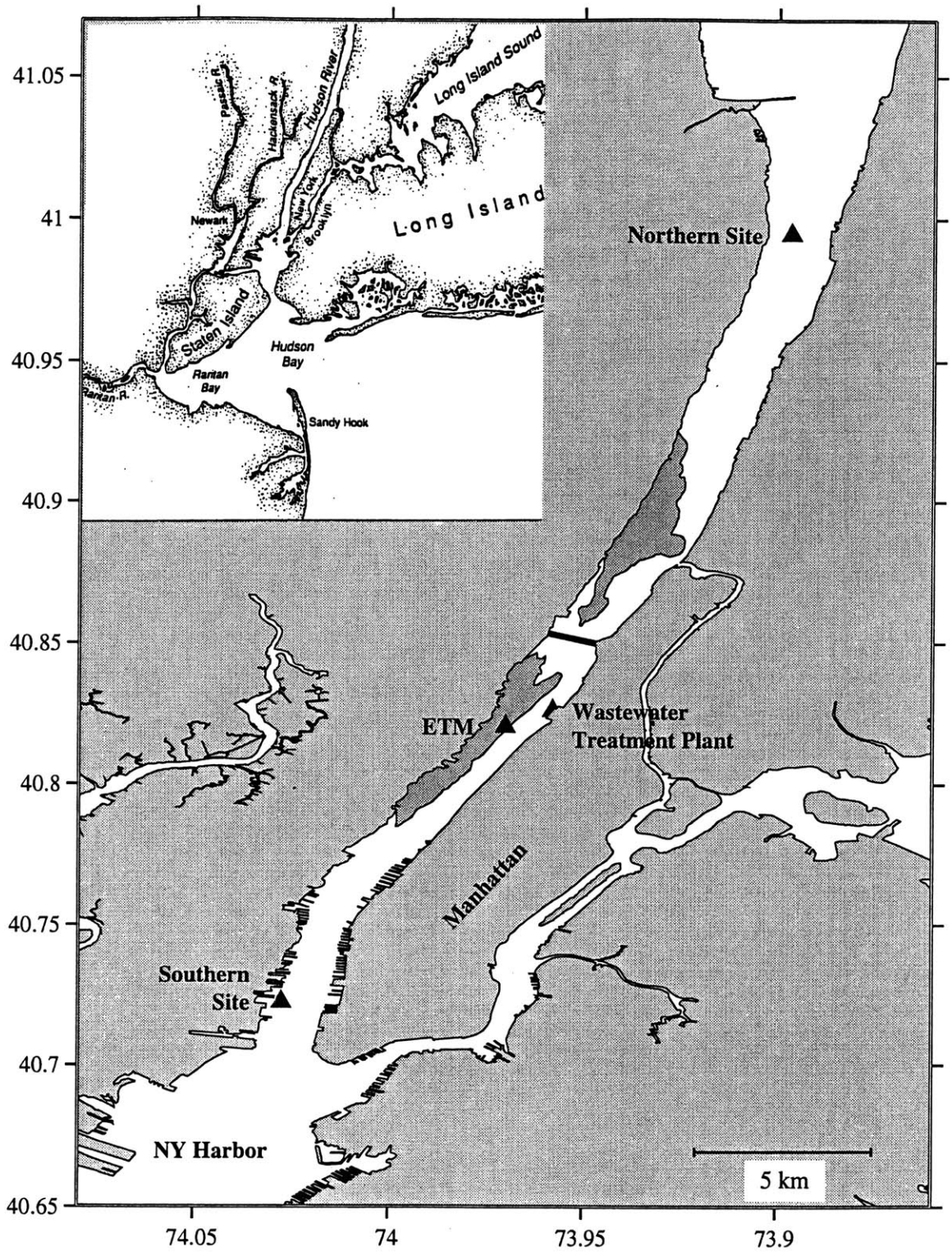

Figure 3.1. Map of the lower Hudson Estuary showing the three sampling stations. Figure created by Steve Margulis.

Figure 3.2. Near-bottom velocity and suspended sediment at the Estuarine Turbidity Maximum in the lower Hudson Estuary.
(Geyer et al., 1999)

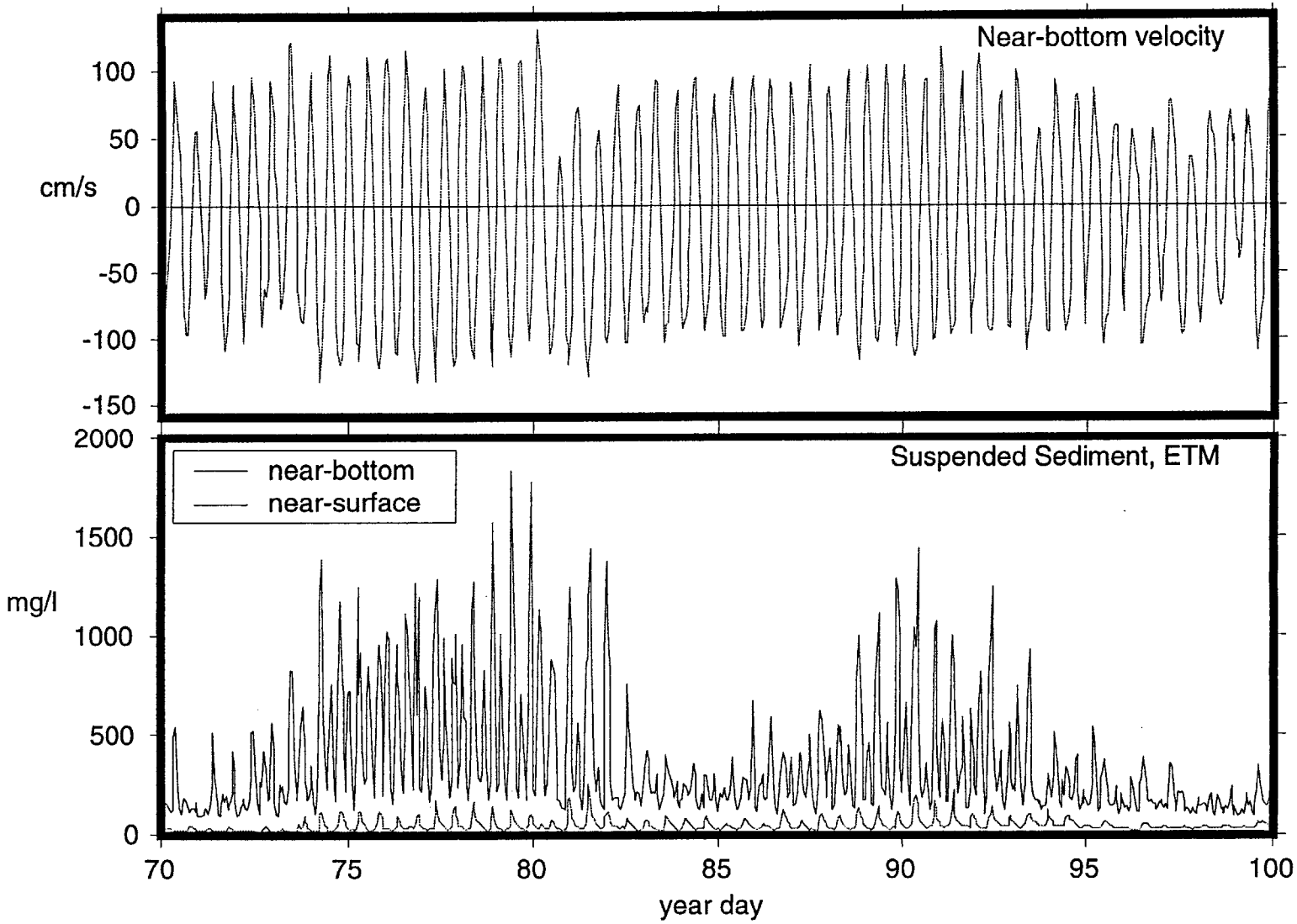
Near-bottom velocity
cm/s
100
50
0
-50
-100
-150
Suspended Sediment, ETM
near-bottom
near-surface
mg/l
2000
1500
1000
500
0
70
75
80
85
90
95
100
year day

METHODS

Field Sampling

PEDs

Polyethylene devices were deployed in the lower Hudson Estuary during two sampling trips. The first was during the neap tide (April 9 – 11, 1999), and the second was during the spring tide (April 15 – 18, 1999). The same three sites were sampled with PEDs during both the neap and spring tides (Figure 3.1). PEDs were deployed at the Southern Site at the southern tip of Manhattan on the western side of the river, at the estuarine turbidity maximum (ETM) approximately 13 km up the river on the western side, and on the western side of the river at the Northern Site which is approximately 34 km up the river from the Battery (Table 3.1).

Two different types of polyethylene were used in the field. One of them was the same used in the lab, manufactured by Brentwood Plastics Inc. (74 to 84 μm thick). The second was manufactured by Carlisle Plastic, Inc. (Minneapolis, MN). This polyethylene was between 51 and 57 μm thick. The PEDs used in the field were 2.5 cm wide, 86 cm long, and approximately 79 μm or 54 μm thick depending on the manufacturer. Prior to deployment, the PEDs were extracted with methylene chloride ($MeCl_2$) twice. Four PEDs were placed in a 500-mL glass bottle filled with JT Baker Ultra-resi analyzed $MeCl_2$ for at least 2 days. And the process was repeated. They were then dried in a laminar flow hood for a minimum of 6 hours. After drying, the PEDs were stored in amber glass jars with screw-on, teflon-lined polypropylene covers. The night before deployment, the PEDs were each punctured with a piece of methylene chloride-rinsed, 16-gauge, stainless steel wire in an accordion manner and stored in a 1 gallon Ziploc bag (Figure 3.3).

Once the boat was anchored, and the engine had been turned off, the stainless steel wire with the PEDs was attached to a nylon rope. The nylon rope was anchored to the bottom and kept vertical with a float. PEDs were attached to the rope so that they would be approximately 1.5, 2.5, 3.5, and 5.5 m from the bottom. The depths for each PED are listed in Table 3.2. A final PED was attached approximately 3 m from the surface. The plastic bags were left around the PEDs until just before the each PED went into the water.

Extra PEDs were also taken into the field and handled on deck in the same manner that the deployed PEDs were in order to determine the PAHs present in the air that would also be in contact with the PEDs that were deployed in the water. While the buoy for the PED deployment was being lowered into the water, the blank PED was exposed to the air. As this PED was exposed for the duration of the buoy deployment (approximately 15 minutes), the blank was exposed longer than each of the water-sampling PEDs was.

The PEDs were deployed for between approximately 2 and 3 days (Table 3.3). At recovery, the rope was lifted from the water with a winch, and as soon as the each PED left the water, it was removed from the wire and placed in a glass amber jar with a teflon-lined polypropylene screw lid.

Table 3.1. Sampling stations and coordinates

Station	Coordinates	
Southern Site (Battery)	40° 43.350' N	74° 01.666' W
Estuarine Turbidity Maximum (ETM)	40° 49.231' N	73° 58.210' W
Northern Site (Hastings)	40° 59.680' N	73° 53.799' W

Table 3.2. PED deployment depths (meters from river bottom).

Station	Neap Tide	Spring Tide
Southern Site (Battery)	9, 3, 1	10, 3.5, 1.5
Estuarine Turbidity Maximum (ETM)	6.7, 3, 1	8.0, 3.5, 1.5
Northern Site (Hastings)	8.5, 3, 1	8, 3, 1

Table 3.3. Length of time for PED deployment (days)

	Length of Deployment (days)	
Station	Neap Tide	Spring Tide
Southern Site (Battery)	2.90	3.13
Estuarine Turbidity Maximum (ETM)	2.79	2.88
Northern Site (Hastings)	3.00	1.96

Water Sampling

Water samples were collected during the second sampling trip (April 15 – 18, 1999). Water samples were collected at the Southern Site, at the Estuarine Turbidity Maximum (ETM), and at the Northern Site. The sampling coordinates were the same as the PED deployment locations (Table 3.1). The Northern Site near Hastings was sampled during maximum flood or incoming tide. The Estuarine Turbidity Maximum was sampled during maximum ebb or outgoing tide. In addition to the vertical profile collected during maximum ebb, a sample was collected at the same site 1 meter off the bottom during flood tide. A sample was also collected 1 meter from the surface next to the North River Wastewater Treatment Plant (Figure 3.1). The Southern Site was sampled during maximum flood or incoming tide. In addition to the vertical profile taken at this site, a water sample was collected 1 meter off of the bottom during ebb tide.

A positive-displacement, gear-driven pump (SP-300; Fultz Pumps, Inc., Lewistown, PA) attached to a water quality multiprobe was lowered over the side of the boat, and samples were collected at approximately 1, 2, and 3 meters off of the bottom and approximately 3 m from the surface. The exact depths sampled for each site are listed in Table 3.4. The water was pumped through $MeCl_2$-rinsed, ¼"diameter, aluminum tubing and collected in $MeCl_2$-rinsed, 1-liter amber glass bottles for later PAH analysis. A second sample for "dissolved" and particulate organic carbon analysis was pumped into 300 mL, clear glass, glass-stoppered, BOD bottles pre-combusted at 450°C. The tops of the bottles were kept covered with aluminum foil to avoid any addition of organic carbon not from the sample.

Clean water was taken on the cruise so that it could be handled on the boat and serve as a blank. Previous to the cruise, the water was reverse osmosis pretreated and run through an ion-exchange resin and activated carbon filter system (Aries Vaponics, Rockland, MA) until a resistance of 18 MΩ was achieved. The water was then treated with ultraviolet light (Aquafine TOC reduction unit, Valencia, CA) and filtered with a 0.22 μm filter (Millipore).

Within 6 hours, approximately 50 mL of $MeCl_2$ were added to each of the 1-liter amber bottles in order to begin extraction and kill any biota present. At the same time a recovery standard consisting of d10-phenanthrene, p-terphenyl, and d12-perylene in hexane was added to each 1-liter sample. At the end of each day, approximately 100 mL of the water from each of the 300-mL samples for organic carbon analysis was filtered using a hand-pumped vacuum with pre-combusted 4.25-cm glass fiber filters (Whatman International Ltd., Springfield Mill, England). The filters

were folded and wrapped in aluminum foil and kept frozen until they could be analyzed for particulate organic carbon (POC). Approximately 3 mL of hydrochloric acid (JT Baker Ultrex II Ultrapure Reagent) was added to the remainder of the sample for later "dissolved" organic carbon analysis. All samples were stored in ice until they could be stored in the laboratory cooler at 4°C.

As mentioned previously, the water-displacement pump was attached to a water quality multiprobe (DataSonde 4; Hydrolab Corporation, Austin, TX). This probe allowed us to measure the following parameters at the time of sampling: depth, temperature, conductivity, turbidity, dissolved oxygen, pH, and chlorophyll concentration. However, the turbidity probe broke at the beginning of our second sampling trip, so we were only able to collect turbidity data for a few of the samples collected during the second trip; these were from the Southern Site.

Table 3.4. Hydrographic data and water sampling depths
(meters measured from surface; only hydrographic data for neap tide).

Station	Neap Tide	Spring Tide
Southern Site (Battery)	1.8, 9.5, 10.5	2.0, 6.9, 7.9, 8.0, 8.9
Estuarine Turbidity Maximum (ETM)	___	3.0, 5.3, 6.3, 7.3
Northern Site (Hastings)	2.1, 9.5, 10.5	3.0, 6.7, 7.7, 8.7

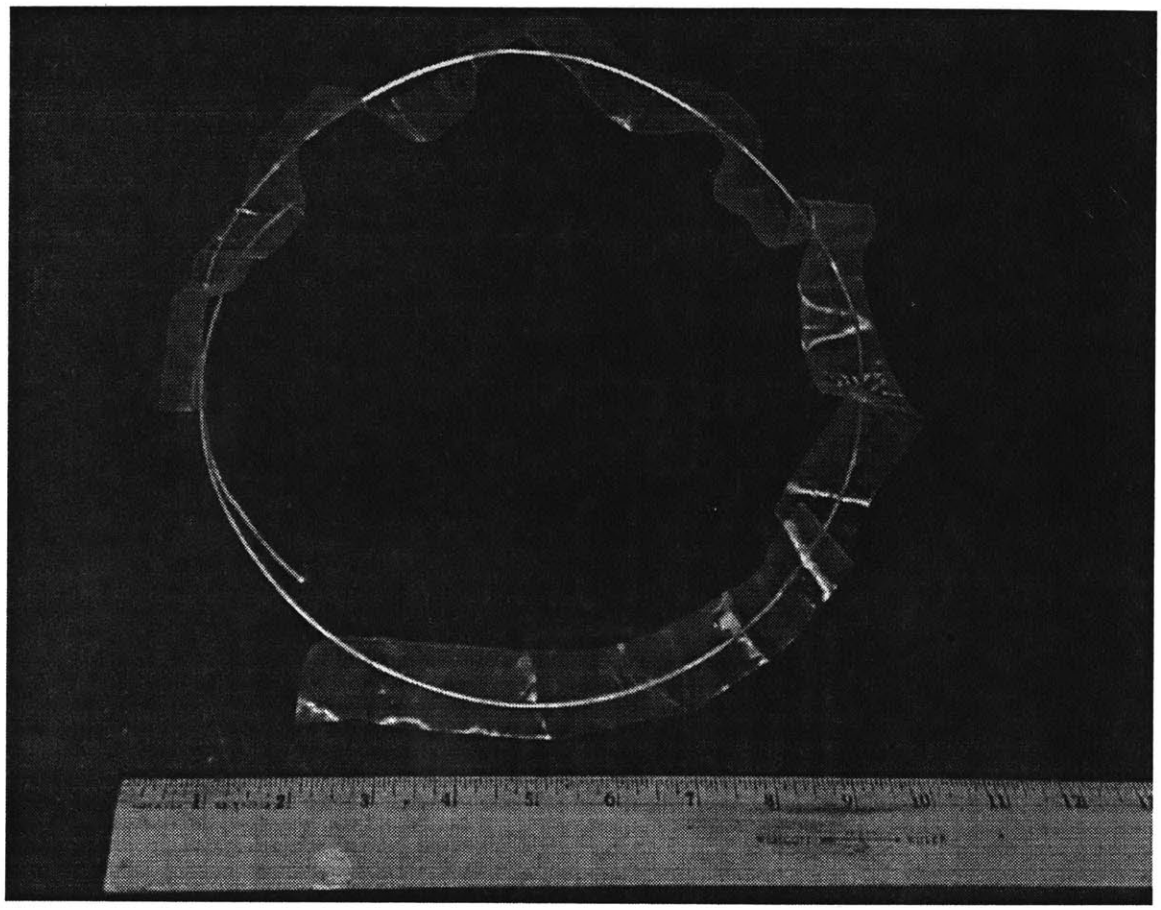

Figure 3.3. Polyethylene device (PED) ready for deployment.

Sample Extraction

PED Extraction

The PEDs were stored in the glass amber jars at 0°C until they were extracted. Each PED was placed in 500 mL of $MeCl_2$ (JT Baker Ultra-resi-analyzed) in glass-stoppered bottles. The bottles were covered with foil to prevent photodegradation. For the PEDs from the second sampling trip, each bottle was spiked with a recovery standard (d10-phenanthrene, p-terphenyl, and d12-perylene). Unfortunately, this recovery standard was not added to the PEDs from the first trip. The bottles were kept in a laminar flow hood. After 1 week, the solvent solution was transferred to a 500 mL round-bottom flask. Between 5 and 10 grams of combusted anhydrous sodium sulfate (Na_2SO_4) were added in order to remove any water that may be present. The flasks were shaken to allow for Na_2SO_4 contact and stored overnight at 0°C. The sample was decanted into a Kuderna-Danish apparatus. The Na_2SO_4 was rinsed with $MeCl_2$ several times, and the rinse was added to the Kuderna Danish. The samples were concentrated to between 2 and 7 mL with the apparatus and transferred to conical vials. Once in the vials, the samples were blown down with N_2 to between 100 and 500 µl. An internal standard (d14-p-terphenyl) was added in order to allow for calculating the volume of the sample. In addition, the vials were weighed before and after the samples were added; this allowed for the calculation of the volume gavimetrically as well.

Water Sample Extraction

The 1-liter water samples were added to 1-liter separatory funnels. Approximately 50 mL of $MeCl_2$ were added, and the funnel was shaken for 3 minutes. The organic solvent and water phases were allowed to separate, and the $MeCl_2$ phase was taken off the bottom into a 500-mL round-bottom flask. This process was repeated twice more. Then pre-combusted anhydrous

Na_2SO_4 was added to the sample, shaken, and stored in the freezer (0°C) overnight in order to remove any water or particulate matter left in the sample. At this point the samples were processed in the same manner that the PED extract samples had been processed.

PAH Analysis and Quantification

The samples were analyzed for polycyclic aromatic hydrocarbons (PAHs) on a gas chromatograph (GC)/mass spectrometer (MS). The GC is a Hewlett Packard 6890 Series with a J&W Scientific DB-5 column. Splitless injection was used, and the GC was temperature programmed from 70°C to 180°C at 20°C/min continued at 6°C/min to 260°C, and finally went to 280°C at 20°C/min. The MS is a JEOL MS-GCmate with electron impact ionization and a magnetic sector analyzer. The recoveries for each of the deuterated standards were calculated for each of the water and PED samples. The recoveries for each sample and deuterated standard were then calculated (Table 3.5).

When recovery standards were added, the reported PAH concentrations were recovery corrected. The recoveries for d10-phenanthrene were used to correct phenanthrene and methylphenanthrene concentrations; p-terphenyl recoveries were used to correct pyrene concentrations; and d12-perylene recoveries were used to correct benzo(a)pyrene concentrations. For the PEDs from the first sampling trip, average deuterated compound recoveries (Table 3.5) were used to correct the reported PAH concentrations.

After the blank water samples were extracted and analyzed, the phenanthrene was not detected and was less than one-quarter of the smallest mass of phenanthrene detected in any of the samples. The same was true for methylphenanthrene. The pyrene-detected mass was 14 times smaller than the

smallest mass of pyrene detected in any sample, and the benzo(a)pyrene was not detected and was less than one-ninth of the smallest mass of benzo(a)pyrene detected in any sample.

The PED blanks for methylphenanthrene, pyrene and benzo(a)pyrene were less than the masses extracted from the PEDs. The smallest methylphenanthrene mass measured in a sample was over twelve times the mass measured in the blank. For pyrene, the smallest sample measured was over 35 times the mass measured in the blank. For benzo(a)pyrene, the smallest mass measured in a sample was over six times the mass measured in the blank. Phenanthrene was a little more problematic. Presumably, because it is more volatile, air contamination of the PEDs by phenanthrene was a problem. For phenanthrene, the smallest mass measured was about two times the mass measured in the blank. All of the phenanthrene and methylphenanthrene samples were corrected for the blanks.

The concentrations of dissolved PAHs present in the water column were calculated using their respective polyethylene-water partition coefficients (K_{PE}; Table 2.3) and temperature-adjusted diffusivities for each chemical (Table 2.4; Diffusivity from Eqn. 2.1). This method is presented in Chapter 2. The polyethylene-water partition coefficient for benzo(a)pyrene was estimated by plotting the phenanthrene and pyrene log K_{PE} values as a function of the log of the octanol-water partition coefficient, fitting a line to these points, and using the K_{OW} for benzo(a)pyrene to estimate a K_{PE}. The correlation from a plot of the natural logarithm of diffusivity vs. the natural logarithm of molar volume (Figure 2.13) was used to estimate the diffusivity of benzo(a)pyrene in polyethylene. This value was then adjusted for the field water temperature with the Arrhenius

equation using an activation energy of 45 kJ/mol (the activation energy estimated for phenanthrene and pyrene in Chapter 2).

Table 3.5. Average PAH recoveries ± 1σ.

Sample Type	Recovery Standard		
	d10-phenanthrene (%)	p-terphenyl (%)	d12-perylene (%)
Water Sample	73 ± 24 (n=17)	69 ± 23 (n=17)	77 ± 29 (n=17)
PED	79 ± 24 (n=12)	97 ± 15 (n=12)	138 ± 21 (n=12)

Particulate Analysis

Total Suspended Solids Analysis

Because the turbidity probe broke during the second sampling trip, the filtered water samples were used to estimate the total suspended solids (TSS). Each folded filter was transferred to a new aluminum foil envelope as the salt in the samples had begun to corrode the foil. The filters in their new envelopes were first weighed, and then placed in a small utility oven (Model 1300U; VWR Scientific, So. Plainfield, NJ) at 71°C in order to dry. They were weighed each of the two following days until they had reached a constant weight indicating that they were dry. The average weight of five different clean filters was used to subtract from the total weight to calculate the mass of solids present. In order to correct for the additional mass of the salt present, water was added to a pre-weighed, clean filter until it was saturated. The mass of the pre-weighed filter was subtracted from the saturated filter mass in order to calculate the mass of water present at saturation. The density of water was used to calculate the volume of water present, and using the

salinity of the water, the additional mass due to salt was calculated. The salt mass was estimated to be between 12 and 87 % of the total suspended solid mass (including salt).

POC Analysis

The dried filter was subsampled with a 4 mm-diameter cork-borer. The subsamples were added to tared silver capsules (D2029, 8 x 5 mm; Elemental Microanalysis Ltd., Manchester, NH) and weighed using an electrical microbalance (Cahn 25 Automatic Electrobalance; Ventron Corp., Cerritos, CA). In order to remove inorganic carbon, low-carbon water and 1 M HCl were added directly to the capsules following the procedure outlined by Gustafsson et al. (1997). The samples were analyzed with a PE 2400 CHN elemental analyzer (Perkin Elmer Corp., Norwalk, CT). The instrument detection limit was approximately 3 μg of C per input. Response factors were determined using an acetanilide standard. The relative standard deviation of these response factors within batches was ± 0.3%. Blanks were prepared for each batch of samples; the average blank was 4.7 ± 1.2 μg of C (n=5).

Soot Analysis

Portions of the remaining dried filter samples were added to preweighed and low-carbon-water rinsed porcelain crucibles with a silica glazed surface (Coors Ceramics, Golden, CO). The soot analysis procedure developed by Gustafsson et al. (1997) was used to remove the non-soot organic carbon. The crucibles with filters were placed into a muffle furnace (Thermolyne Model F-A1730) equipped with an auxiliary temperature controller (Thermolyne Furnatrol 133, Sybron Corp., Dubuque, IA) and covered with precombusted aluminum foil. The samples were oxidized in the presence of excess oxygen (air) for 24 hours at 375°C. After the samples had cooled, the same

method outlined above for the removal of inorganic carbon was followed, and the samples were analyzed with the PE 2400 CHN analyzer just as the POC samples were.

RESULTS AND DISCUSSION

Hydrographic Data

The lower Hudson Estuary was observed to be more stratified during the neap tide than during the spring tide. This is illustrated by the observed salinity profile (Figure 3.4; Geyer et al., 1999). During the neap tide, there was a significant vertical salinity gradient at all stations. During the spring tide, there was less of a vertical gradient, and it became less distinct moving up the river toward the north. Temperature profiles also indicated vertical variation (Table 3.6). There was greater vertical variability during neap tide, especially at the Northern Site.

An increase in total suspended solids (TSS) was observed between neap and spring tides (Figure 3.4). Total suspended solids ranged from 8 to 40 mg/L during neap tide and from 20 to 400 mg/L during spring tide. During spring tide, suspended solids increased with increasing depth suggesting that the sediment bed is the primary source for these suspended solids. Particulate organic carbon (POC) measurements ranged from 3 to 12 mg/L. The average concentration of POC at the ETM was 9 mg/L, while the average measured POC concentration at the Southern Site was 4 mg/L. Soot concentrations ranged from 0.11 to 0.30 mg/L.

Table 3.6. Vertical temperature gradient (from bottom to top; °C)

Station	Length of Deployment	
	Neap Tide (°C)	Spring Tide (°C)
Southern Site (Battery)	7.20 – 7.40	8.33 – 8.48
Estuarine Turbidity Maximum (ETM)	___	9.06 – 9.10
Northern Site (Hastings)	7.96 – 8.76	9.46 – 9.41

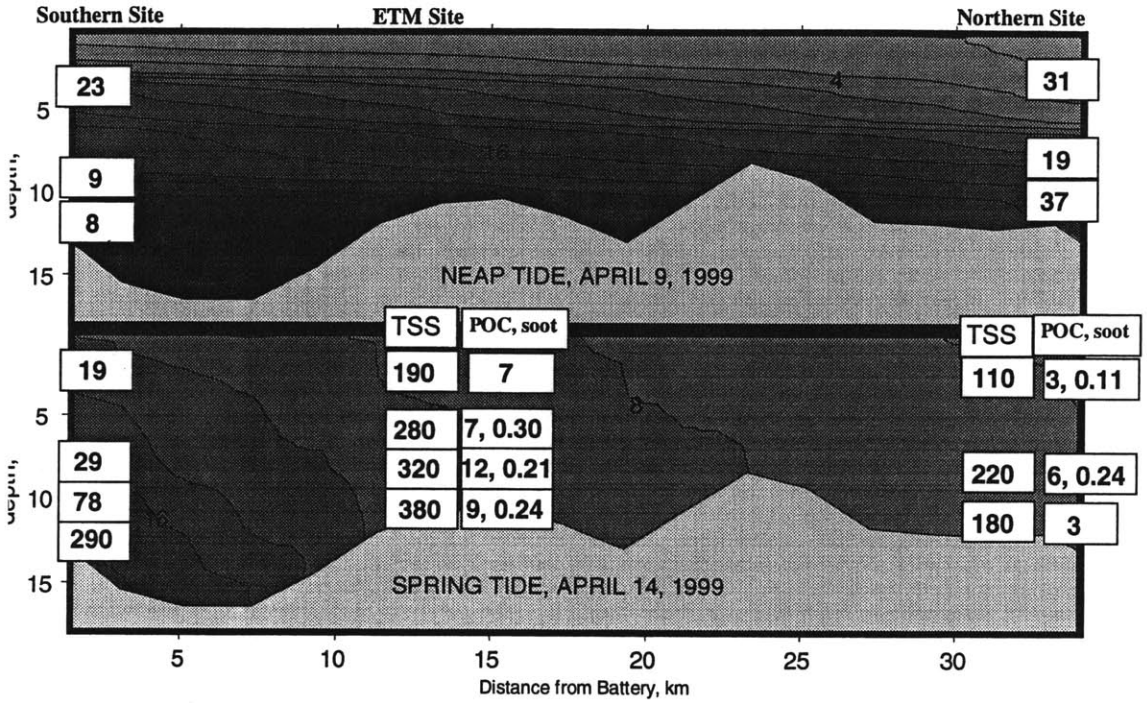

Salinity in practical salinity units (psu)
Neap Tide Depths (meters from surface): Northern: 1.8, 9.5, 10.5; Southern: 1.8, 9.5, 10.5
Spring Tide Depths (meters from surface): Northern: 3, 6.7, 7.7, 8.7; ETM: 3, 5.3, 6.3, 7.3; Southern: 2, 6.9, 7.9, 8,

Figure 3.4. Total suspended solids, particulate organic carbon (POC) and soot (mg/L) during neap and spring tides in the lower Hudson Estuary.

Total and Dissolved PAH Concentrations

The total concentrations (mass of chemical extracted from water sample including particles) of phenanthrene, pyrene, and benzo(a)pyrene measured in the water column during spring tide was found to be significantly higher than the dissolved concentrations of phenanthrene, pyrene, and benzo(a)pyrene (Figures 3.5-3.7). For phenanthrene, the total mass (dissolved and sorbed) was between 1.3 and 100 times the dissolved mass. The total mass of pyrene was between 1 and 50 times the dissolved mass, and the total benzo(a)pyrene concentration was between 3300 and 33,000 times the dissolved concentration. This illustrates the large difference between the "truly dissolved" and total PAH concentration. As the dissolved fraction has been observed to be more immediately bioavailable than the sorbed fraction (McElroy et al., 1990), the dissolved portion is of toxicological concern. However, once this dissolved fraction has been removed, a portion of the sorbed concentrations will desorb in order to equilibrate with the water. Consequently, the large concentrations of PAHs present are also a concern.

In most cases, there were larger total PAH concentrations near the river bottom; there were also higher total suspended solids and particulate organic carbon (POC) measured near the river bottom. The differences in PAH concentrations between the top and bottom of the water column were most noticeable at the Southern and Northern sites. The estuarine turbidity maximum PAH concentrations appeared to be much more uniform vertically.

The total PAH (dissolved and particulate) mass per mass of particles present in the water collected one meter off the bottom of the river were calculated (Table 3.7). This allowed for the comparison of total (dissolved and particulate) PAH results with measurements collected from other studies of

the lower Hudson Estuary (Wolfe et al., 1996 and Mitra et al., 1999). The measurements completed for this study were compared with the concentrations of phenanthrene and pyrene present in sediments samples from the East River and Newark Bay (Mitra et al., 1999) and phenanthrene present in sediments throughout the Hudson-Raritan Estuary (Wolfe et al, 1996). The range of phenanthrene and pyrene concentrations measured in this study is within the range reported by Mitra et al. (1999). In contrast, Wolfe et al. (1996) measured average phenanthrene concentrations much larger than ours. However, the highest values they measured were in the East River, which was not sampled for this study.

Table 3.7. Concentrations of particle-sorbed PAHs measured in the lower Hudson Estuary.

Chemical	This Study (ng/g)	Mitra et al., 1999 (ng/g)	Wolfe et al., 1996 (ng/g)
Phenanthrene	100 – 700 average: 300	East River: 1000 Newark Bay: 100	400 – 200,000 average: 6000
Pyrene	300 – 2000 average: 300	East River: 2000 Newark Bay: 600	—

Peven et al. (1996) measured PAHs in *Mytilus edulis* in the Hudson-Raritan Estuary; however, they did not estimate dissolved concentrations that would correspond to the concentrations measured in the mussel. To our knowledge the dissolved concentrations of PAHs in the lower Hudson River estuary have not been measured or estimated from measurements. However, because of the ubiquitous nature of PAH sources (fossil fuel and wood combustion and petroleum spills) we would expect that the concentrations measured in the Hudson would be similar (within an order of magnitude) to the PAH concentrations measured in other urban bodies of water. Lebo

et al. (1992) used semipermeable membrane devices (SPMDs) to measure PAHs in an urban creek in Missouri. Flores (1998) also used SPMDs to measure phenanthrene and pyrene in Boston Harbor. Our phenanthrene and pyrene values are similar (same order of magnitude) to the values measured by Lebo et al. (1992) and Flores (1998; Table 3.8). Our benzo(a)pyrene values are within an order of magnitude of the concentrations measured by Lebo et al. (1992). The dissolved PAH concentrations in the lower Hudson River appear to be lower than those concentrations measured in inner Boston Harbor and the urban creek in Missouri.

Table 3.8. Dissolved concentrations measured in three different urban bodies of water.

Chemical	This Study Lower Hudson River (ng/L)	Lebo et al., 1992 Urban Creek in Missouri (ng/L)	Flores, 1998 Boston Harbor (ng/L)
Phenanthrene	0.4 - 5	9	5 - 40
Pyrene	0.5 - 10	12	6 - 60
Benzo(a)pyrene	0.001 – 0.05	0.3	___

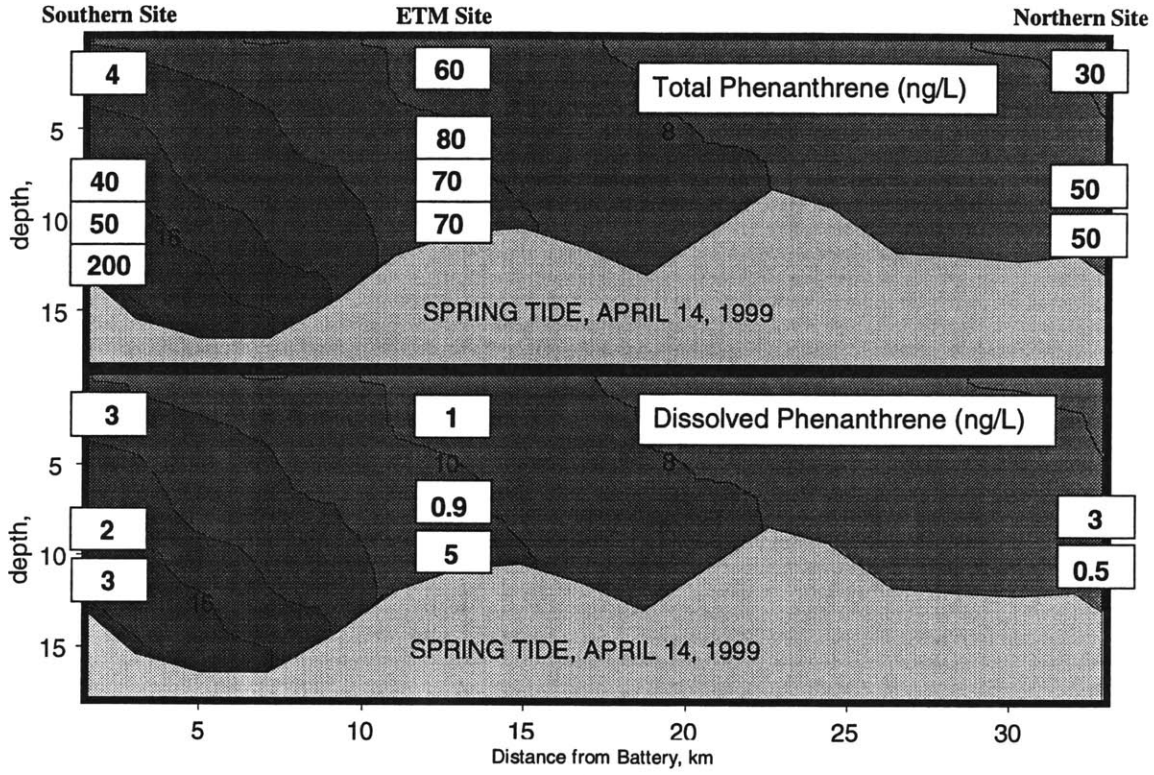

Salinity in practical salinity units (psu)
Total PAH Depths (meters from surface): Northern: 3, 7.7, 8.7; ETM: 3, 5.3, 6.3, 7.3; Southern: 2, 6.9, 7.9, 8.9
Dissolved PAH Depths (meters from bottom): Northern: 3, 1; ETM: 8, 3.5, 1.5; Southern: 10, 3.5, 1.5

Figure 3.5. Total and dissolved phenanthrene (ng/L) in the lower Hudson Estuary.

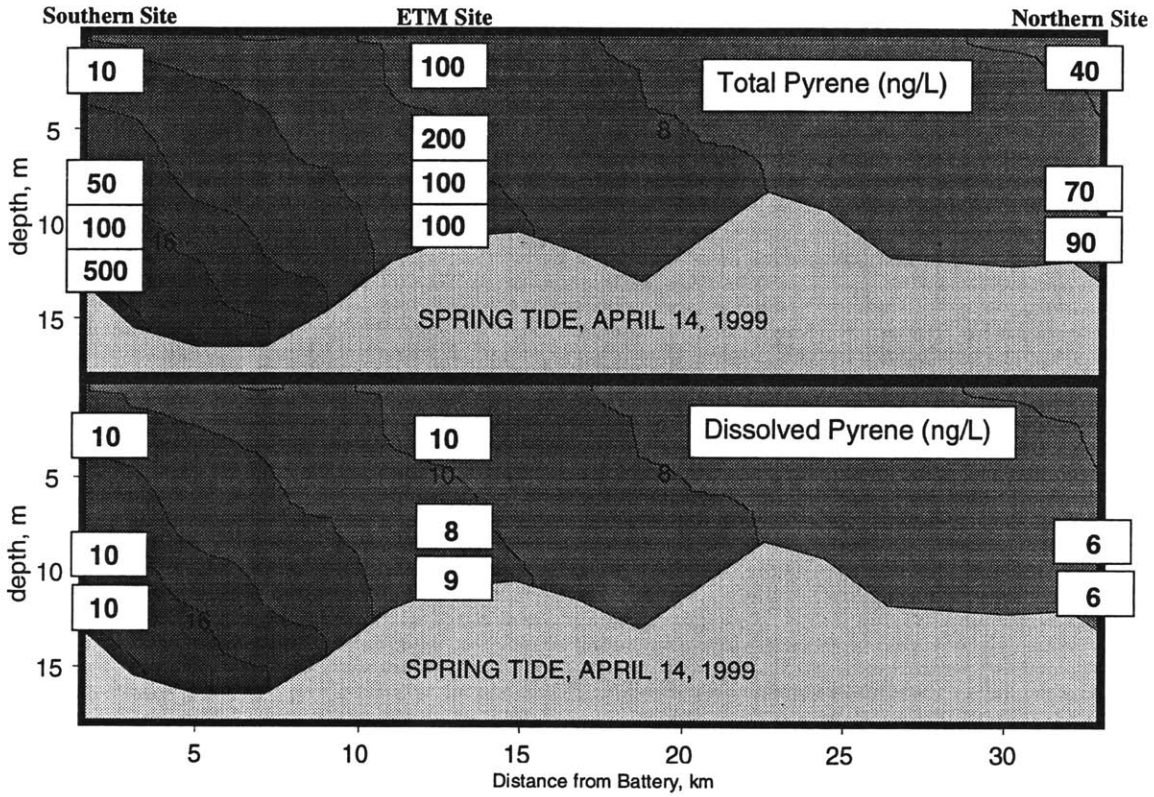

Salinity in practical salinity units (psu)
Total PAH Depths (meters from surface): Northern: 3, 7.7, 8.7; ETM: 3, 5.3, 6.3, 7.3; Southern: 2, 6.9, 7.9, 8.9
Dissolved PAH Depths (meters from bottom): Northern: 3, 1; ETM: 8, 3.5, 1.5; Southern: 10, 3.5, 1.5

Figure 3.6. Total and dissolved pyrene (ng/L) in the lower Hudson Estuary.

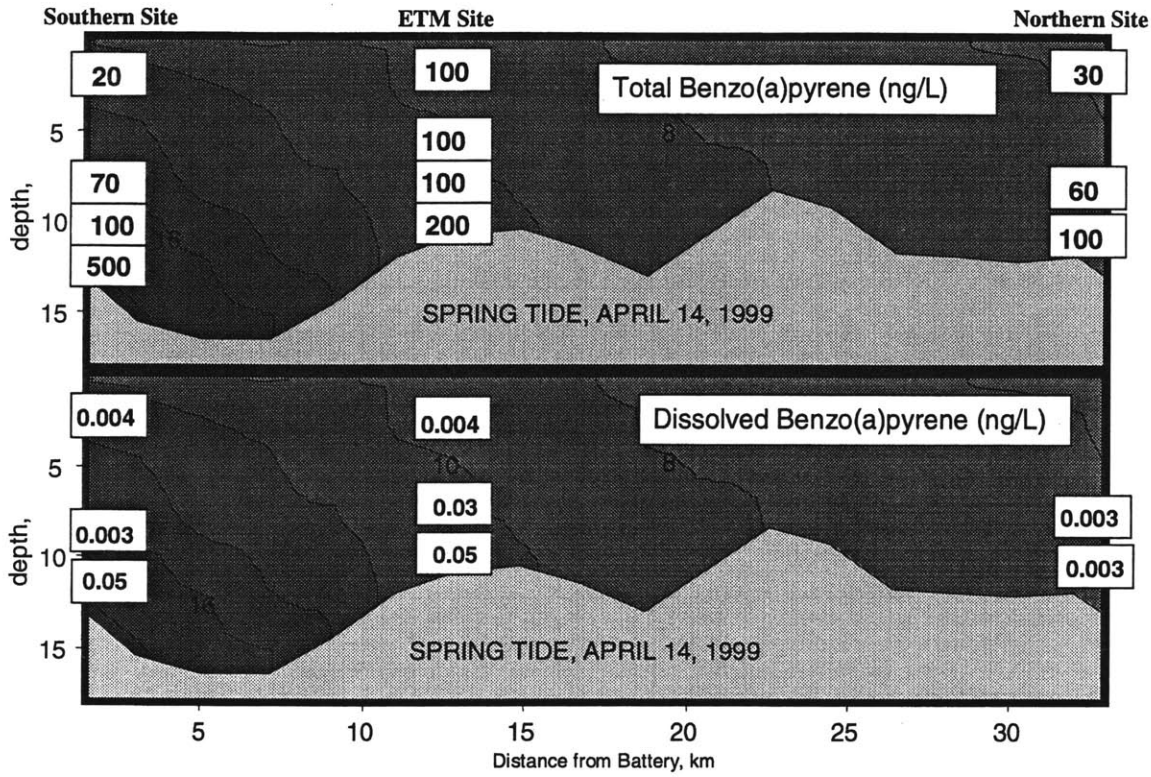

Salinity in practical salinity units (psu)
Total PAH Depths (meters from surface): Northern: 3, 7.7, 8.7; ETM: 3, 5.3, 6.3, 7.3; Southern: 2, 6.9, 7.9, 8.9
Dissolved PAH Depths (meters from bottom): Northern: 3, 1; ETM: 8, 3.5, 1.5; Southern: 10, 3.5, 1.5

Figure 3.7. Total and dissolved benzo(a)pyrene (ng/L) in the lower Hudson Estuary.

Temporal Variability

The tidal influences to the lower Hudson Estuary make it a dynamic and changing water body. Consequently, it is important to examine temporal variations in PAH concentrations. The Southern Site was sampled, 1 meter off the bottom, during both maximum flood and ebb (Table 3.9). Samples were also collected at the estuarine turbidity maximum (ETM) during maximum flood and ebb. At both locations, samples collected during maximum flood contained higher concentrations of phenanthrene, pyrene, and benzo(a)pyrene than samples collected during maximum ebb. Phenanthrene concentrations were between three and four times greater. Pyrene concentrations were about five times greater, and benzo(a)pyrene concentrations were between two and eight times greater during the maximum flood tide. These observed increases could be due to increased resuspension during the flood tide. They may also indicate a greater source of PAHs coming from the harbor than from upriver. This theory may be supported by the high PAH concentrations measured by Wolfe et al. (1996) in the East River which empties into the harbor at the tip of Manhattan.

Table 3.9. Total PAH concentrations during maximum flood and ebb.

Sampling Site	Flood			Ebb		
	Phen. (ng/L)	Pyrene (ng/L)	B(a)p (ng/L)	Phen. (ng/L)	Pyrene (ng/L)	B(a)p (ng/L)
ETM (~ 1 m off bottom)	300	500	400	70	100	200
Southern site (~ 1 m off bottom)	200	500	500	60	90	60

Observed and Predicted Dissolved Fractions

The observed (measured) and predicted dissolved PAH fractions were compared by first, estimating the fraction of phenanthrene, pyrene, and benzo(a)pyrene dissolved in the water column at equilibrium. The measured water fraction was calculated by dividing the dissolved PAH concentration (measured with PEDs) by the total (dissolved and sorbed) PAH concentration. Assuming only dissolved and sorbed-to-filterable particle species, one may derive an express for f_w, the fraction of chemical in the water (Schwarzenbach et al., 1993):

$$f_w = \frac{1}{1 + r_{sw} \cdot K_D} \tag{3.1}$$

where r_{sw} is the ratio of solid to water (M/L^3) and K_D is the solid-water distribution ratio (L^3/M). K_D was calculated in two ways. In one case, the K_D was calculated considering only organic matter as a partitioning medium:

$$K_D = f_{om} \cdot K_{om} \tag{3.2}$$

where f_{om} is the fraction of organic matter (estimated as 2 times the fraction of organic carbon), and K_{om} is the organic matter-water partition coefficient.

Using this model, the predicted dissolved phenanthrene fraction was between 7 and 34 times greater than the measured water fraction (Figure 3.8a). For pyrene, this model over-predicted the dissolved fraction by between 4 and 24 (Figure 3.8b). The predicted benzo(a)pyrene dissolved fractions were between 180 and 11,000 times greater than the measured fractions (Figure 3.8c). These differences in measured and predicted values may indicate that the system is far from equilibrium or that a better estimate for the solid-water distribution ratio is needed.

Gustafsson et al. (1997) have proposed an alternate method for estimating particle-water partition coefficients which attempts to include PAH partitioning to soot in addition to organic matter partitioning:

$$K_D = f_{om} \cdot K_{om} + f_{sc} \cdot K_{ac} \qquad (3.3)$$

where f_{sc} is the fraction of soot carbon and K_{ac} is activated carbon-water partitioning coefficient.

Using this equation for estimating the dissolved water fraction, the predicted dissolved fraction of phenanthrene was between two and ten times greater than the measured fraction (Figure 3.8a). The average predicted dissolved fraction of phenanthrene predicted including soot partitioning in the model was six times greater than the measured dissolved fraction. For pyrene, the predicted dissolved fraction was between two and six times the measured fraction (Figure 3.8b). The average predicted fraction was three times the measured value. For benzo(a)pyrene, the predicted fraction was between 45 and 2900 time the dissolved fraction measured (Figure 3.8c). The average predicted fraction was 650 times greater than the average fraction measured. It is important to note that soot carbon-water partition coefficients have not been measured and that activated carbon-water partition coefficients were used as an estimate. The activated carbon-water partition coefficients were estimated from calculations by Gustafsson et al. (1997) based on studies by Walters and Luthy (1984; log K_{ac}'s: phenanthrene—6.8; pyrene—7.1; benzo(a)pyrene—8.2). These estimates for the soot carbon-water partition coefficients may be off by as much as an order of magnitude. Consequently, estimating K_D with Equation (3.3) may result in poor predictions and account for or contribute to the poor correlations between predicted and observed water fractions. However, the predicted values vary greatly from the measured values, especially for benzo(a)pyrene.

These results suggest that the PAHs sorbed to suspended particles and dissolved in the water column were not in equilibrium. There are several possible explanations for this. The suspension time of the particles may not be sufficient for the PAHs to equilibrate with the surrounding water. Because the total PAH samples are collected at a single point in time, and the dissolved fraction is a time-averaged value, it is likely that the total PAH sample was not representative of the three-day average. In fact, the total PAH samples were collected during times of high resuspension when larger concentrations are expected; this would likely contribute to the under estimation of the measured dissolved fraction. Once PAHs have desorbed from particles, they may be bio- or photo-degraded. They may diffuse into the air. All of these may contribute to the large disequilibrium. As the Hudson River's net flow is seaward, the desorbed particles may be flushed from the system before equilibrium can be reached. Finally, as discussed by McGroddy et al. (1996), some of the PAHs may be tightly bound to soot and unavailable for equilibrium partitioning.

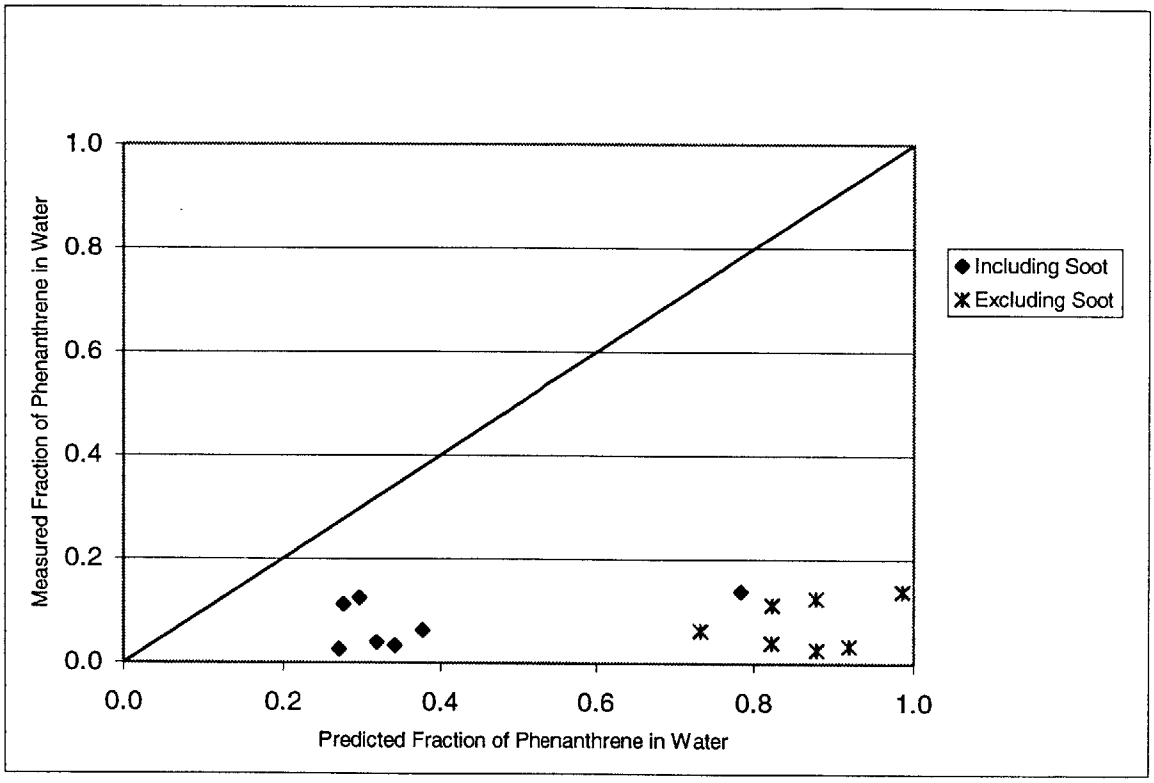

Figure 3.8a. Measured f_w vs. predicted f_w for phenanthrene.

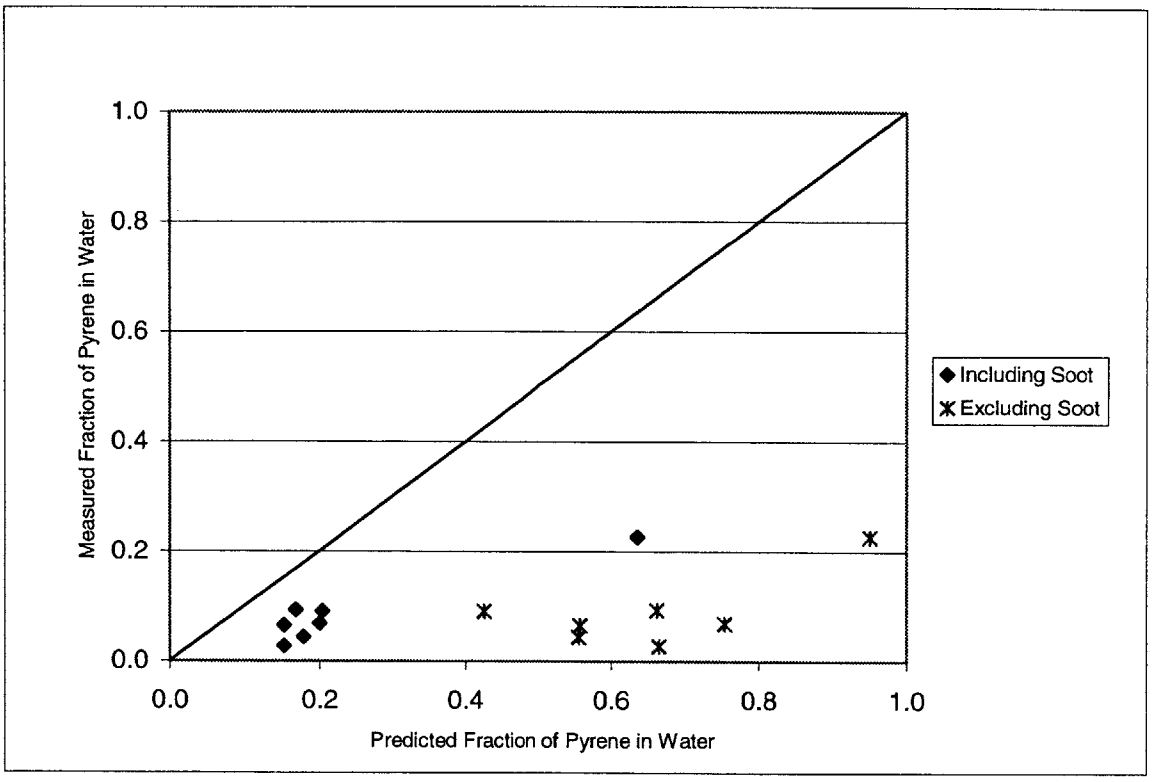

Figure 3.8b. Measured f_w vs. predicted f_w for pyrene.

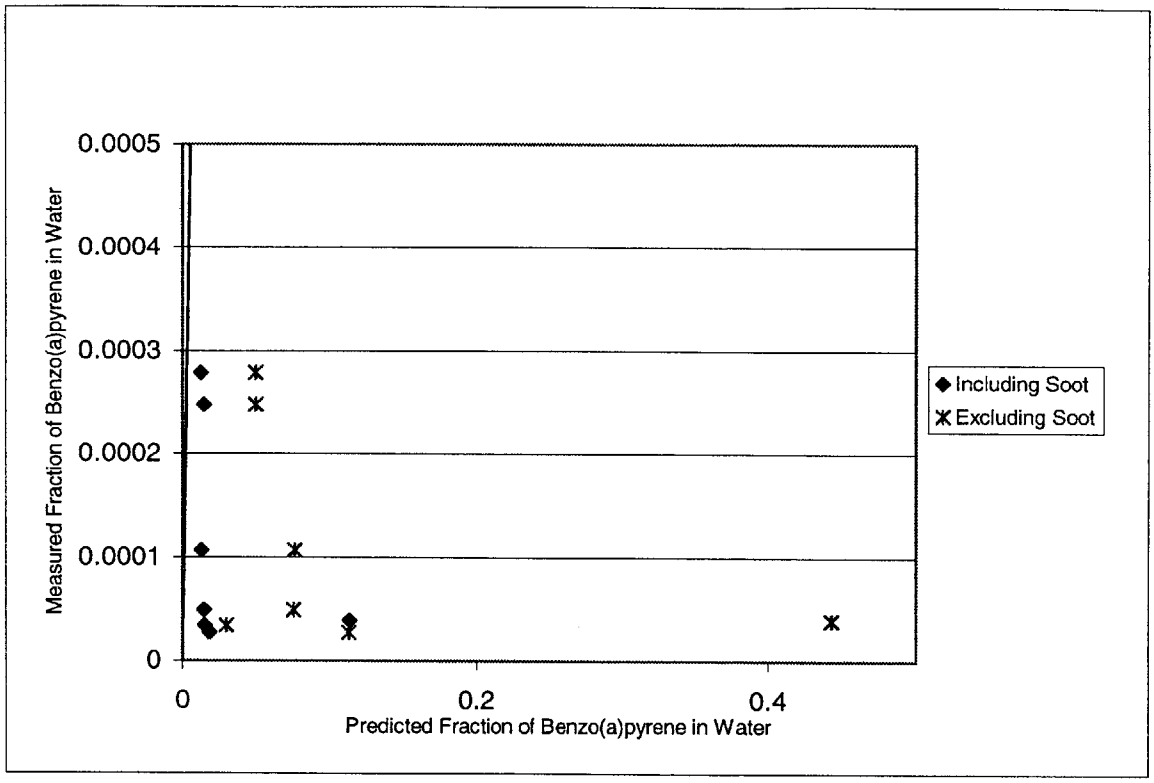

Figure 3.8c. Measured f_w vs. predicted f_w for benzo(a)pyrene.

Time for Desorption

A possible explanation for the apparent disequilibrium between the sorbed and aqueous PAHs may be a residence time which is smaller than the required desorption time. Geyer et al. (1999) estimated that during spring tide, the lower Hudson Estuary residence time is between 2 and 3 days. Due to the tidally correlated resuspension events, four resuspension events are expected each day. (A resuspension event is expected during each of the two maximum flood events per day and during each of the maximum ebb events per day.) Assuming that the particles were suspended for an hour during each event, it is estimated that the particles were suspended for approximately 4 hrs/day. Assuming a spring tide residence time of 2.5 days, the overlying water would have been exposed to 10 hours of particle resuspension. So, if a chemical's time for equilibrium desorption was less than 10 hours, one would expect the sorbed and aqueous PAHs to be in equilibrium.

Under infinite bath conditions, Schwarzenbach et al. (1993) estimate the time for 50% of desorption equilibrium:

$$t_{50\%} \cong 0.03 \cdot R^2 \cdot \frac{K_d^*(1-\phi)\rho_s + \phi}{\phi \cdot f \cdot D_w} \tag{3.4}$$

and the time for desorption equilibrium (five half-lives):

$$t_{equilibrium} \cong 0.3 \cdot R^2 \cdot \frac{K_d^*(1-\phi)\rho_s + \phi}{\phi \cdot f \cdot D_w} \tag{3.5}$$

where

R: average particle radius (L)

K_d^*: in situ (microscopic) distribution coefficient (L^3/M)

ϕ: porosity

ρ_s: particle density (M^3/L)

f: tortuosity factor

D_w: diffusivity of chemical in water (L^2/T)

The in situ distribution coefficient was estimated:

$$K_d^* \cong f_{OC} \cdot K_{OC} \qquad (3.6)$$

where f_{oc} is the fraction of organic carbon, and K_{oc} (L^3/M) is the organic carbon-water partition coefficient. When the above parameters had not been measured, they were estimated (Table 3.10). Diffusivity in water and the in situ distribution coefficient were estimated for phenanthrene, pyrene, and benzo(a)pyrene (Table 3.11). Using the estimated and measured parameters, the times for 50% of equilibrium and equilibrium desorption for phenanthrene, pyrene, and benzo(a)pyrene were estimated using Equations (3.4) and (3.5); Table (3.12). For phenanthrene, the estimated time of water column contact with suspended sediments was between the time for 50% of desorption equilibrium (5 hr) and the time for desorption equilibrium (50 hr). This result supports the finding that sorbed phenanthrene is not in equilibrium with the aqueous phenanthrene. For pyrene, both of the time for desorption estimates were greater than the estimated time for water column contact. The time for 50% of desportion equilibrium was estimated to be 20 hours, while the time for desorption equilibrium was 200 hours. This calculation supports the finding that sorbed pyrene is not in equilibrium with the aqueous pyrene. The estimated desorption time for benzo(a)pyrene ranged from 500 hours (50% of desorption equilibrium) and 5000 hours (desorption equilibrium). These desorption times are much greater than the estimated time of water and suspended solid contact. This finding agrees with the significant observed disequilibrium between sorbed and aqueous benzo(a)pyrene.

Both the time for desorption and the time of water and suspended particle contact are estimates based on several assumptions. It is possible that these estimates are only good to an order of magnitude; however, the estimated times for desorption agree with the observed aqueous and sorbed PAH disequilibrium.

Table 3.10. Measured and estimated parameters for calculating desorption time.

Parameter	Value	Measured or Estimated
Particle radius, R (m):	1E-4	Estimated
Fraction organic carbon, f_{oc}:	0.05	Measured
Bulk density, $\rho_s(1-\phi)$ (kg/m^3):	2000	Estimated
ϕ*f:	0.02	Estimated

Table 3.11. Estimated diffusivity in water and in situ distribution coefficient for calculating desorption time.

Chemical	D_w (m^2/s)	K_d* (m^3/kg)
Phenanthrene	7E-10	0.4
Pyrene	6E-10	2
Benzo(a)pyrene	5E-10	40

Table 3.12. Desorption time for 50% of equilibrium and equilibrium.

Chemical	Time for 50% of equilibrium (hours)	Time for equilibrium (hours)
Phenanthrene	5	50
Pyrene	20	200
Benzo(a)pyrene	500	5000

Source for Dissolved PAHs

Examining the chemical signal of the dissolved fraction may allow one to determine the source of this fraction. If the sediments are indeed a significant source for this dissolved fraction, one would expect the characteristics of the dissolved and total PAH samples to be similar. For example, the ratio of phenanthrene-to-methylphenanthrene for #2 fuel oil is approximately 0.03 (Pancirov and Brown, 1975), while this ratio is 3.0 for a firwood fire (combustion source; Lee et al., 1977) and 1.6 for Boston air (Gschwend and Hites, 1981), which would also primarily represent a combustion source. These measurements indicate that methylated phenanthrenes are relatively more abundant in oils and much less abundant in combustion-derived sources.

In order to investigate if resuspended sediments are a source of PAHs to the water column, the ratio of phenanthrene-to-methylphenanthrene was calculated for the dissolved fraction and the total water column fraction. The total water column sample was predominantly composed of particle-bound PAHs. The phenanthrene/methylphenanthrene ratio for the dissolved fraction samples (measured with PEDs) during spring tide ranged from 0.13 to 1.1. The average ratio was 0.39 ±

0.29 (Figure 3.9a; Table 3.13). Dissolved samples (measured with PEDs) collected during neap tide show similar phenanthrene/methylphenanthrene ratios; they ranged from 0.06 to 0.71, and the average ratio was 0.31 ± 0.17 (Figure 3.9b; Table 3.13). Although the increase observed between the neap and spring tide ratio was within the standard deviation, the neap tide samples appear to have a lower ratio, suggesting less of a particulate source. One would expect this because the neap tide produces less particle resuspension than the spring tide. The phenanthrene/methylphenanthrene ratios for the total (sorbed and dissolved) PAH extracts were also calculated (Figure 3.10; Table 3.9). These ratios ranged from 0.96 to 1.75, and the average ratio was 1.25 ± 0.24. These differences in phenanthrene/methylphenanthrene ratios suggest that sorbed PAHs have a larger pyrogenic source than the dissolved PAHs do.

Table 3.13. Dissolved phenanthrene/methylphenanthrene ratio and the calculated fractional input from oil and air source.

Spring Tide

Sample	178/192	f_{oil}	f_{air}
Firwood Fire[a]	3		
Boston Air[b]	1.6		
Lab Blank	2.1		
N Blank	2		
ETM Blank	4.6		
S Blank	2.5		
Northern Site @ 3m	1.1	0.64	0.36
Northern Site @ 1m	0.22	0.93	0.07
ETM @ 8m	0.18	0.95	0.05
ETM @ 3.5m	0.13	0.96	0.04
ETM @ 1.5m	0.53	0.82	0.18
Southern Site @ 10m	0.35	0.89	0.11
Southern Site @ 3.5m	0.35	0.89	0.11
Southern Site @ 1.5m	0.33	0.89	0.11
Kuwait Crude[c]	0.1		
#2 Fuel Oil[c]	0.03		
Average:	0.39	0.87	0.13
Standard Dev.:	0.29	0.10	0.10

Neap Tide

Sample	178/192	f_{oil}	f_{air}
Firwood Fire[a]	3		
Boston Air[b]	1.6		
N Blank	2.1		
ETM Blank	3.0		
Northern Site @ 8.5m	0.3	0.90	0.10
Northern Site @ 3m	0.32	0.90	0.10
Northern Site @ 1m	0.4	0.87	0.13
ETM @ 6.7m	0.06	0.99	0.01
ETM @ 3m	0.15	0.96	0.04
ETM @ 1m	0.19	0.94	0.06
Southern Site @ 9m[d]	0.48	0.84	0.16
Southern Site @ 3m[d]	0.56	0.81	0.19
Southern Site @ 1m[d]	0.71	0.76	0.24
Kuwait Crude[c]	0.1		
#2 Fuel Oil[c]	0.03		
Average:	0.31	0.90	0.10
Standard Dev.:	0.17	0.06	0.06

Oil 172/192: 0.03
Air 172/192: 2.8 +/- 1.0
a Lee et al., 1977
b Gschwend & Hites, 1981
c Pancirov & Brown, 1975
d These ratios were not corrected for a blank as a blank was not sampled on this day.

Spring annd Neap Average:	0.37	0.88	0.12
Standard Dev.:	0.24	0.09	0.09

It has been hypothesized that petroleum hydrocarbons discharged to coastal areas are available for biological uptake to a greater extent than pyrogenic source hydrocarbons (Farrington et al., 1983). The pyrogenic hydrocarbons are believed to be more strongly associated with pyrogenic particles and less bioavailable than petroleum hydrocarbons. PEDs provide an excellent method to test this hypothesis, as those PAHs that are bioavailable would be expected to diffuse into the PED. In order to determine the dominate source for the dissolved fraction, ratios of PAHs present in the PED were compared to both petrogenic and pyrogenic source PAH ratios.

Assuming that the dissolved and total PAH are from a combination of two sources: petrogenic and pyrogenic, one can estimate the fraction that each of these contributes to the dissolved and total PAH masses.

$$M = xO + yA \qquad (3.7)$$

where M is the mixture ratio, x is the fraction of the sample that is from oil, O is the oil ratio (assumed to be 0.03 for #2 fuel oil; Pancirov and Brown, 1975), y is the fraction of the sample from an air or combustion source, and A is the ratio of the average air source at the sites.

It was assumed that the air ratio will be similar to a combustion ratio. The field blanks were averaged resulting in a ratio of 2.8 ± 1.0 (Figures 3.11a and 3.11b). Using Equation (3.7), the fraction of the dissolved samples from oil was calculated and averaged 0.87 ± 0.10 during spring tide and 0.90 ± 0.06 during neap tide (Table 3.13). Approximately 90% of the dissolved phase PAHs appear to be of a petrogenic source. In contrast, the estimated fraction of total samples from oil is 0.56 ± 0.09 and 0.44 ± 0.09 for the air or combustion source (Table 3.14). The phenanthrene/methylphenanthrene ratio decreased as the river flows to the harbor. This suggests

that the total PAH contribution becomes more and more petrogenic as the river flows south. This may be due to increased boat traffic close to the harbor. There are several ferry routes near lower Manhattan.

Table 3.14. Ratio of phenanthrene to methylphenanthrene in the total water column and calculated fractional input from oil and air source.

Sample	178/192	Foil	Fair
Firwood Fire[a]	3		
Boston Air[b]	1.6		
N @ 3 m	1.75	0.38	0.62
N @ 7.7m	1.47	0.48	0.52
N @ 8.7m	1.61	0.43	0.57
ETM @ 3m	1.34	0.53	0.47
ETM @ 5.3m	1.06	0.63	0.37
ETM @ 6.3m	1.19	0.58	0.42
ETM @ 7.3m	1.22	0.57	0.43
ETM @ 9m	1.20	0.58	0.42
ETM @ 8.9m	1.23	0.57	0.43
Sewage Eff. @ 1m	1.33	0.53	0.47
S @ 2m	0.97	0.66	0.34
S @ 7.9m	1.23	0.57	0.43
S @ 8.0m	0.96	0.66	0.34
S @ 8.9m	0.97	0.66	0.34
Kuwait Crude[c]	0.1		
#2 Fuel Oil[c]	0.03		
Average:	1.25	0.56	0.44
Standard Deviation:	0.24	0.09	0.09

Oil 172/192: 0.03
Air 172/192: 2.8 +/- 1.0
a Lee et al., 1977
b Gschwend & Hites, 1981
c Pancirov & Brown, 1975

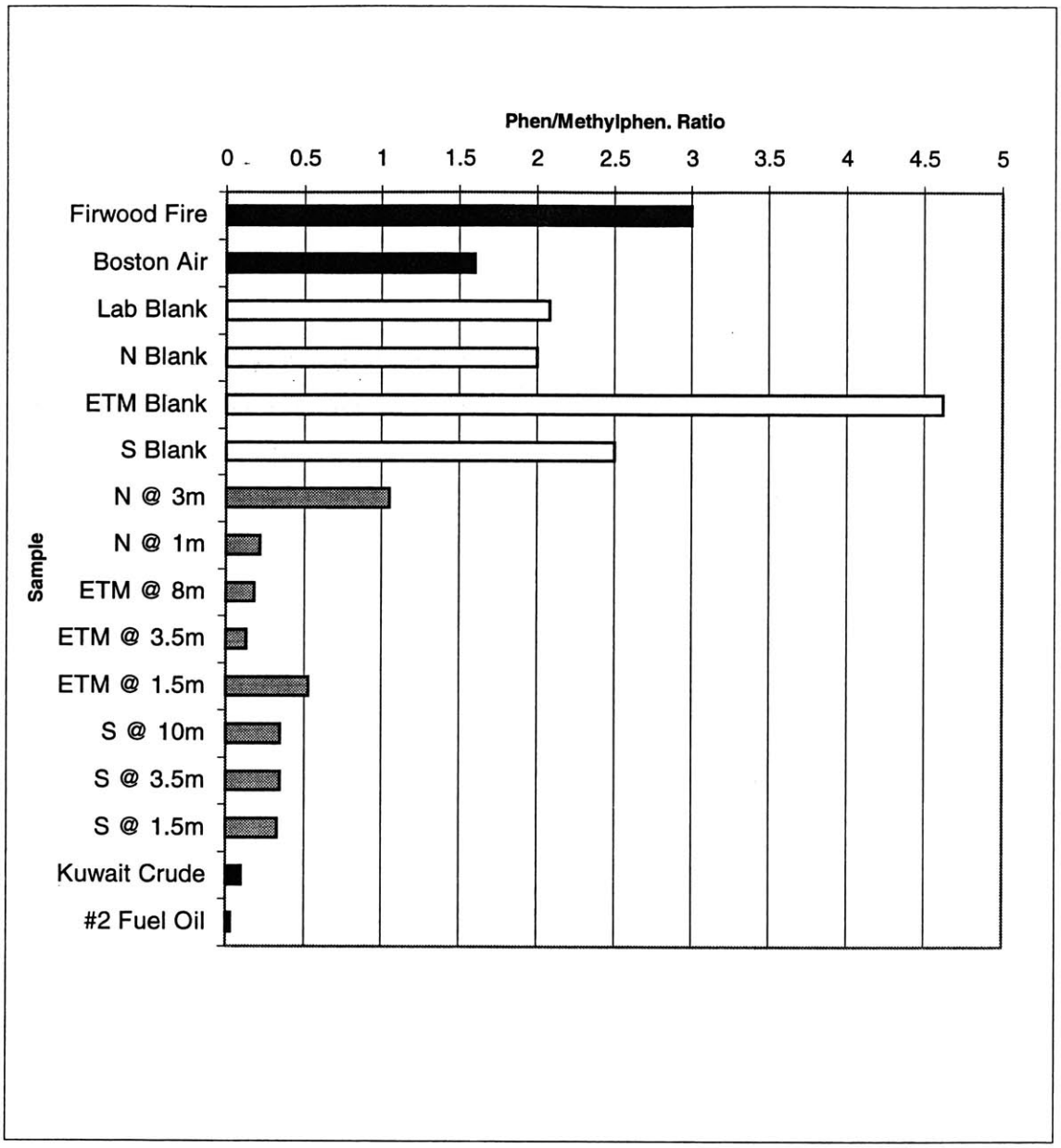

Figure 3.9a. Dissolved phenanthrene/methylphenanthrene ratios (spring tide).

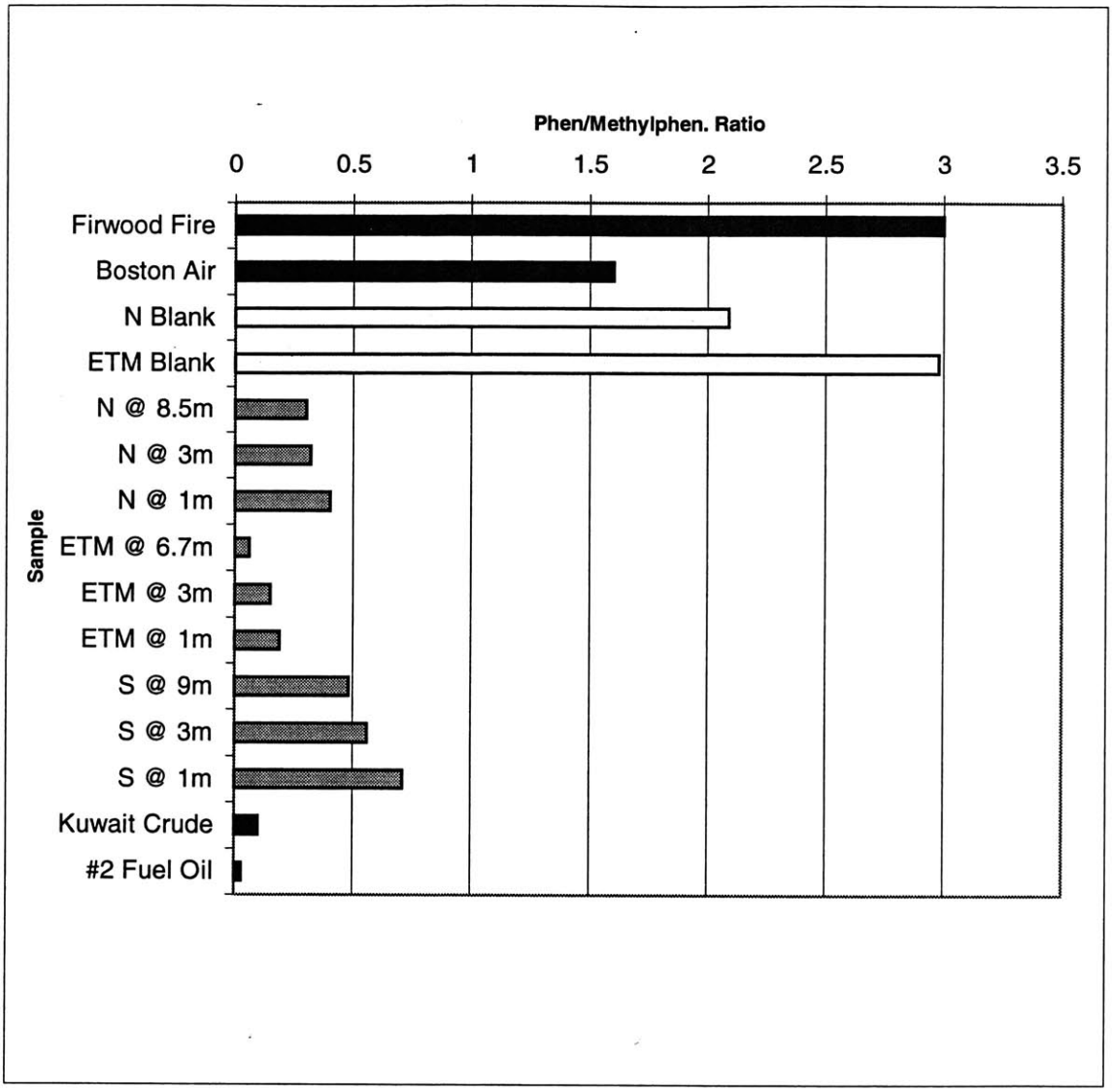

Figure 3.9b. Dissolved phenanthrene/methylphenanthrene ratios (neap tide).

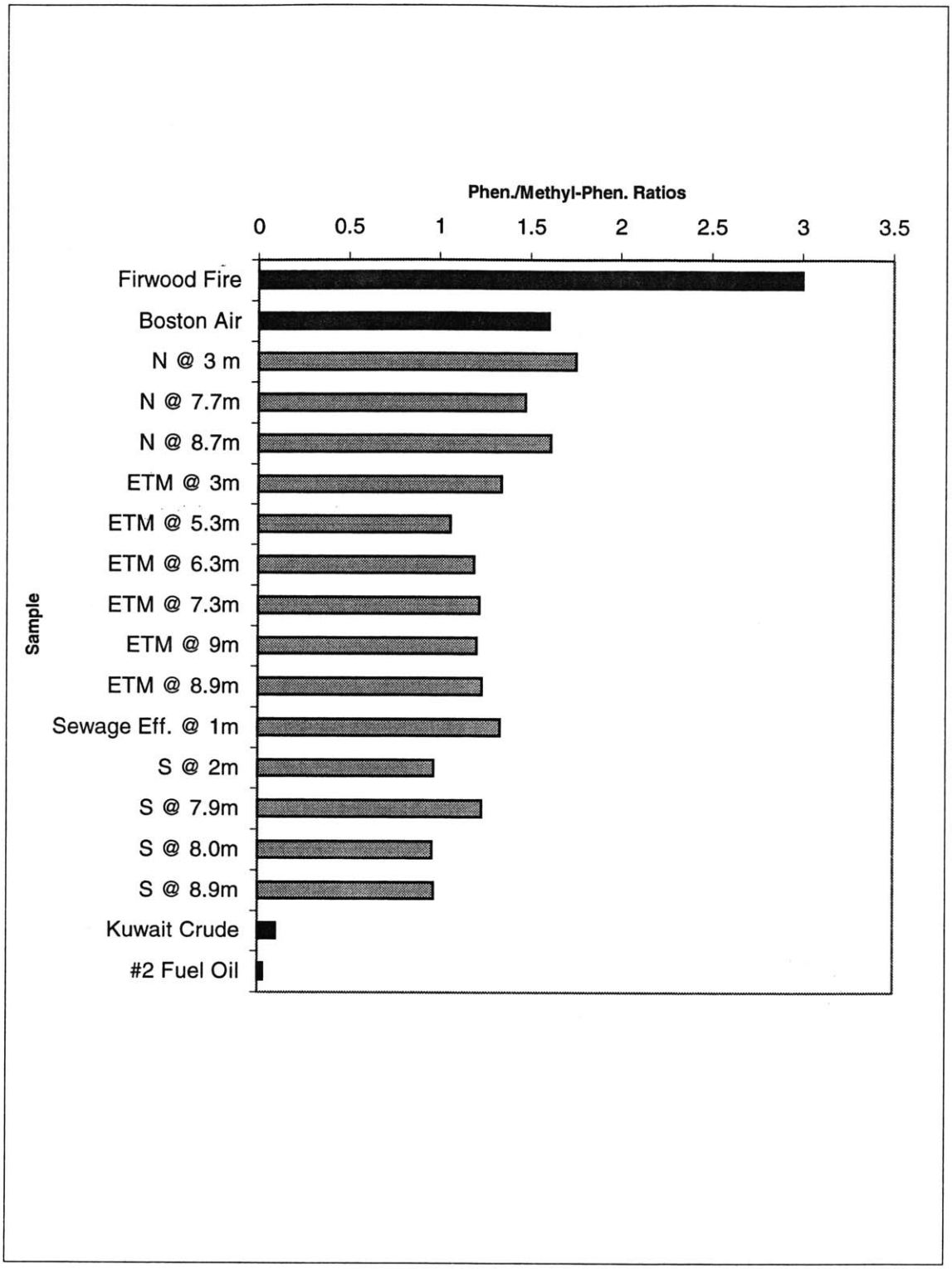

Figure 3.10. Total phenanthrene/methylphenanthrene ratios (spring tide).

Increase in Dissolved PAHs during Increased Resuspension

While the sorbed and aqueous PAHs in the lower Hudson Estuary did not appear to reach equilibrium, there did appear to be an increase in the dissolved concentration for the more hydrophobic PAHs (pyrene and benzo(a)pyrene) during increased sediment resuspension. Dissolved pyrene concentrations increased by factors ranging from 2 to 20 when the tide changed from neap to spring (Figure 3.11). The average concentration increased from 2 to 9 ng/L. Dissolved benzo(a)pyrene concentrations increased during the spring tide by factors as high as 25; however in one case they decreased (Figure 3.12). For benzo(a)pyrene, the average concentration increased from 7 pg/L to 30 pg/L. Dissolved phenanthrene concentrations remained essentially constant between neap and spring tide (Figure 3.13). The average concentration was 2 ng/L during both neap and spring tides. The relatively constant dissolved phenanthrene concentration between neap and spring tides suggests that the aqueous and sorbed phenanthrene may be in equilibrium.

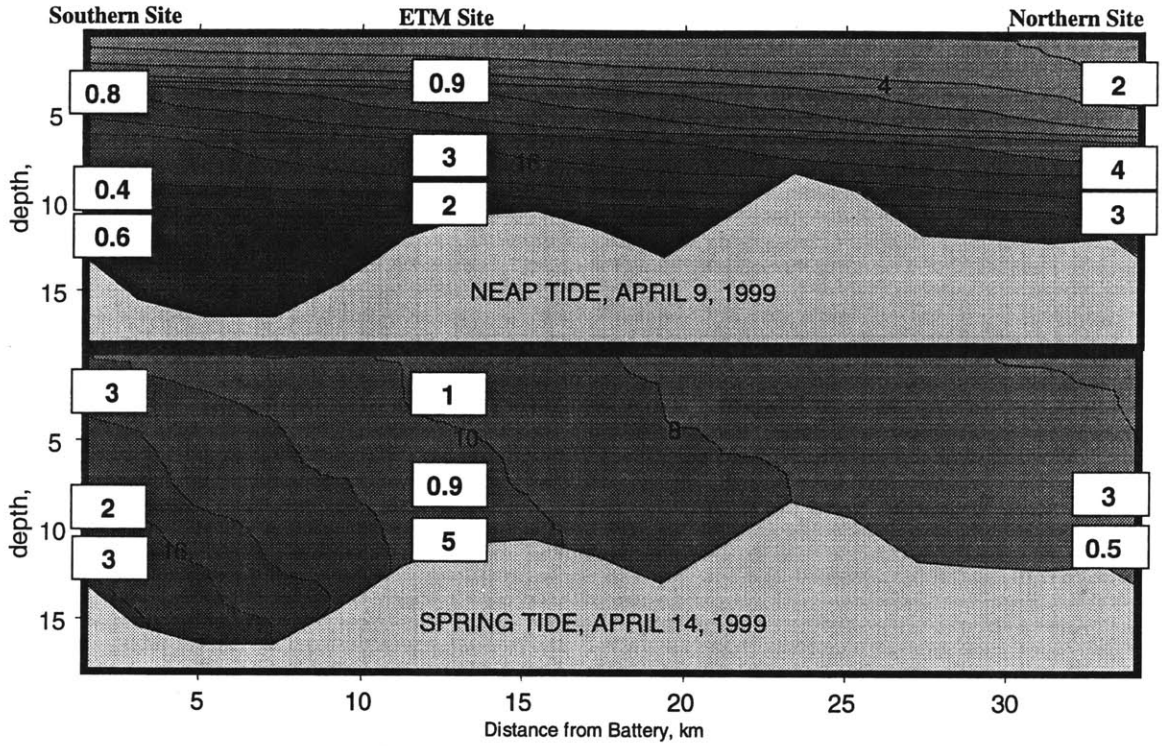

Salinity in practical salinity units (psu)
Neap Tide Depths (meters from bottom): Northern: 8.5, 3, 1; ETM: 6.7, 3, 1; Southern: 9, 3, 1
Spring Tide Depths (meters from bottom): Northern: 8, 3, 1; ETM: 8, 3.5, 1.5; Southern: 10, 3.5, 1.5

Figure 3.11. Dissolved phenanthrene (ng/L) during neap and spring tides in the lower Hudson Estuary.

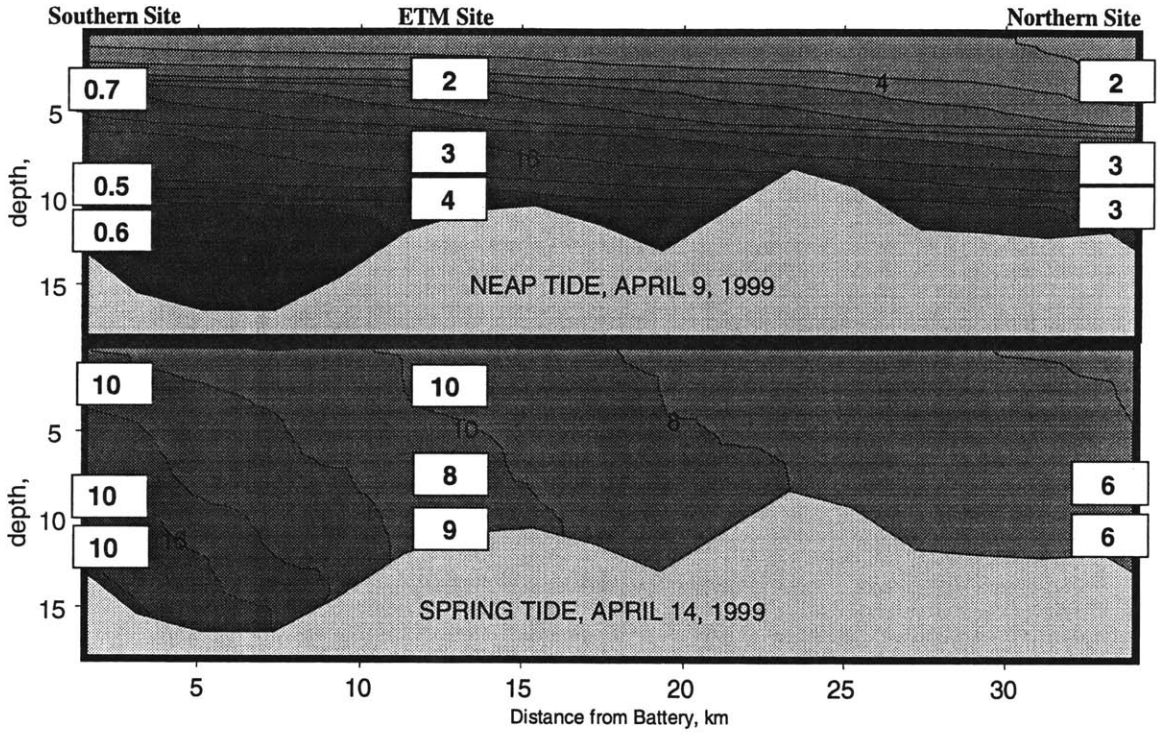

Salinity in practical salinity units (psu)
Neap Tide Depths (meters from bottom): Northern: 8.5, 3, 1; ETM: 6.7, 3, 1; Southern: 9, 3, 1
Spring Tide Depths (meters from bottom): Northern: 8, 3, 1; ETM: 8, 3.5, 1.5; Southern: 10, 3.5, 1.5

Figure 3.12. Dissolved pyrene (ng/L) during neap and spring tides in the lower Hudson Estuary.

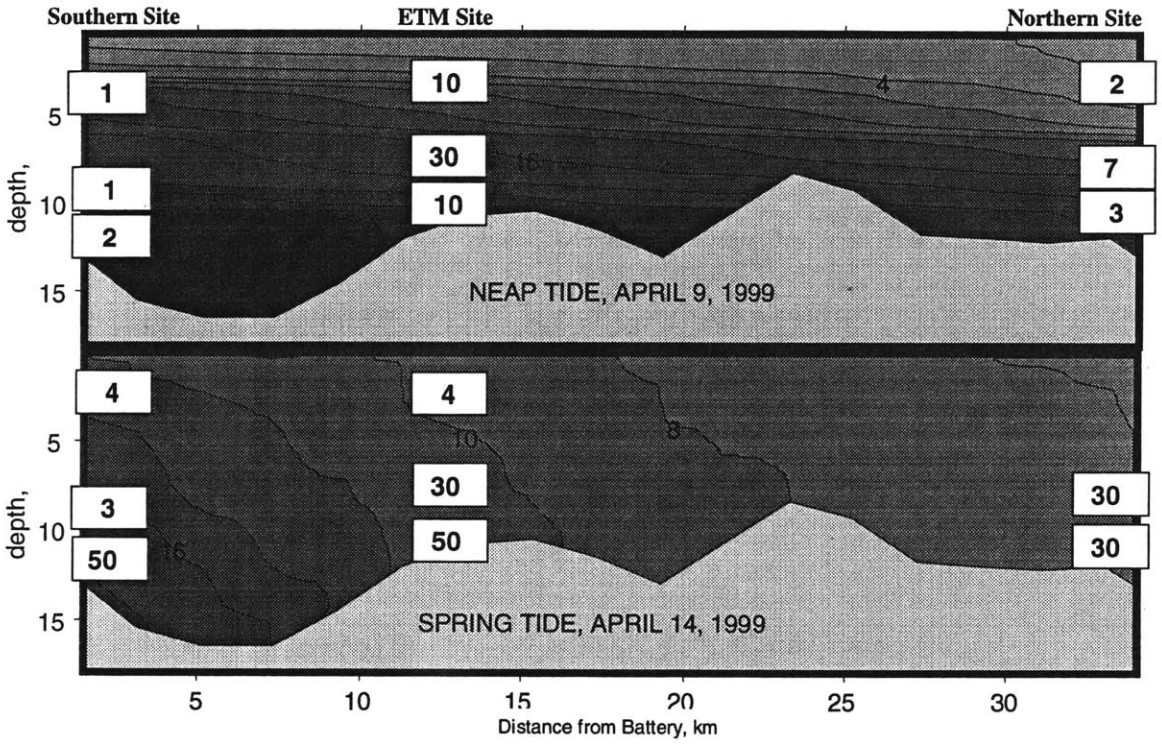

Salinity in practical salinity units (psu)
Neap Tide Depths (meters from bottom): Northern: 8.5, 3, 1; ETM: 6.7, 3, 1; Southern: 9, 3, 1
Spring Tide Depths (meters from bottom): Northern: 8, 3, 1; ETM: 8, 3.5, 1.5; Southern: 10, 3.5, 1.5

Figure 3.13. Dissolved benzo(a)pyrene (pg/L) during neap and spring tides in the lower Hudson Estuary.

CONCLUSIONS

The increased concentration of the more hydrophobic dissolved PAHs (pyrene and benzo(a)pyrene) observed between neap and spring tide suggested that increased particle resuspension resulted in an increase in the dissolved PAH fraction. However, the discrepancy between observed and predicted PAH water fractions suggested that the aqueous and sorbed PAHs were not at equilibrium. Predicted PAH water concentrations were closer to the observed values when PAH partitioning to soot was included in the partitioning model. This suggested that soot does sorb PAHs in the aquatic environment. However, even when soot was included in the model, the suspended solid phase did not fully explain the discrepancies between dissolved values expected from suspended solid concentrations and observed dissolved concentrations. Estimates of the time for PAH desorption during particle suspension indicated that there was not sufficient time for the more sorbed, hydrophobic PAHs (pyrene and benzo(a)pyrene) to equilibrate with the aqueous phase.

The relative abundances of phenanthrene and methylphenanthrene observed in the total PAH pool, which was predominantly particle-bound, were very different from the ratios observed in the dissolved pool. It appeared that approximately 55% of the total (dissolved and sorbed) PAHs were from a petrogenic source, while about 90% of the dissolved PAHs were from a petrogenic source. As the dissolved fraction is believed to be more readily bioavailable, the PAHs from a petrogenic source may be of a greater ecotoxicological concern than those from a pyrogenic source, especially if much of the particle-bound PAHs are irreversibly bound.

REFERENCES

Abood, K. A. 1978. Hudson River hydrodynamic and water quality characteristics: prospectives on the New York Bight Symposium. Williamsburg, VA, November, 5-10, 1978. *As cited in Geyer, 1995.*

Achman, D. R., B. J. Brownawell, and L. Zhang. Exchange of polychlorinated biphenyls between sediment and water in the Hudson River estuary. *Estuaries* **19**, 950-965.

Cooper, J. C., F. R. Cantelmo, and C. E. Newton. 1988. Overview of the Hudson River estuary. *American Fisheries Society Monograph* **4**, 11-24.

Demuth, S., E. Casillas, D. A. Wolfe, and B. B. McCain. 1993. Toxicity of saline and organic solvent extracts of sediments from Boson Harbor, Massachusetts and the Hudson River-Raritan Bay Estuary, New York using the Microtox® Bioassay. *Arch. Environ. Contam. Toxicol.* **25**, 377-386.

Farrington, J. W.; E. D. Goldberg, R. W. Risebrough, J. H. Martin, and V. T. Bowen. 1983. U.S. "Mussel Watch" 1976-1978: An overview of the trace-metal, DDE, PCB, hydrocarbons, and artificial radionuclide data. *Env. Sci. Technol.* **17**, 490-496.

Flores, A. E. 1998. Assessing the Fate of PAHs in the Boston Inner Harbor Using Semipermeable Membrane Devices (SPMDs). Master of Engineering Thesis. Dept. of Civil and Environmental Engineering. MIT. 121 pp.

Geyer, W. R. 1995. Final report: particle trapping the lower Hudson Estuary. Hudson River Foundation, New York, NY, Grant No. 002/92A.

Geyer, W. R., P. M. Gschwend, R. G. Adams. 1999. Sediment-water column exchange of toxic organic compounds. Presentation for Office of Naval Research, Arlington, VA, November 3, 1999.

Gschwend, P. M. and R. A. Hites. 1981. Fluxes of polycyclic aromatic hydrocarbons to marine and lacustrine sediments in the northeastern United States. *Geochim. Cosmochim. Acta.* **45**, 2359-2367.

Gustafsson, Ö, F. Haghseta, C. Chan, J.MacFarlane, and P. M. Gschwend. 1997. Quantification of the dilute sedimentary soot phase: implications for PAH speciation and bioavailability. *Env. Sci. Technol.* **31**, 203-209.

Hirshberg, D. and H. J. Bokuniewicz. 1991. Measurements of water temperature, salinity and suspended sediment concentrations along the axis of the Hudson River estuary 1980-1981, *Special Data Report #11, Reference #91-14*, 38 pp., Marine Science Research Center, State University of New York, Stony Brook, NY. *As cited in Geyer, 1995.*

Karickhoff, S. W. 1984. Organic pollutant sorption in aquatic systems. *J. Hydraulic Engineering* **110**, 707-735.

Lebo, J. A., J. L. Zajicek, J. N. Huckins, J. D. Petty, and P. H. Peterman. 1992. Use of semipermeable membrane devices for in situ monitoring of polycyclic aromatic hydrocarbons in aquatic environments. *Chemosphere* **25**, 697-718.

Lee, M. L., G. P. Prado, J. B. Howard, R. A. Hites. 1977. Source identification of urban airborne polycyclic aromatic hydrocarbons by gas chromatographic mass spectrometry and high resolution mass spectrometry. *Biomed. Mass. Spectrom.* **4**, 182-186.

McElroy, A. E., J. W. Farrington, and J. M Teal. 1990. Influence of mode of exposure and the presence of a tubiculous polychaete on the fate of benz(a)anthracene in the benthos. *Env. Sci. Technol.* **24**, 1648-1655.

McGroddy, S. E., J. W. Farrington, and P. M. Gschwend. 1996. Comparison of the in situ and desorption sediment-water partitioning of polycyclic aromatic hydrocarbons and polychlorinated biphenyls. *Env. Sci. Technol.* **30**, 172-177.

Mitra, S, T. M. Dellapenna, and R. M. Dickhut. 1999. Polycyclic aromatic hydrocarbon distribution within lower Hudson River estuarine sediments: physical mixing *vs* sediment geochemistry. *Estuarine, Coastal & Shelf Science* **49**, 311-326.

Neff, J. M. 1979. *Polycyclic Aromatic Hydrocarbons in the Aquatic Environment*; Applied Science, London. 262 pp.

Pancirov, R. J. and R. A Brown. 1975. Analytical methods for polynuclear aromatic hydrocarbons in crude oils, heating oils, and marine tissues. *Proc. 1975 Conf.* On Prevention and control of oil pollution. 103-113. *As cited in Gschwend and Hites, 1981.*

Petroni, R. N. and P. H. Israelsson. 1998. Mass Balance and 3D Model of PAHs in Boston's Inner Harbor. Master of Engineering Thesis. Dept. of Civil and Environmental Engineering. MIT. 224 pp.

Peven, C. S., A. D. Uhler, R. E. Hillman, W. G. Steinhauer. 1996. Concentrations of organic contaminants in *Mytilus edulis* from the Hudson-Raritan Estuary and Long Island Sound. *The Science of the Total Environment.* **179**, 135-147.

Schwarzenbach, R. P., P. M. Gschwend, and D. M. Imboden. 1993. *Environmental Organic Chemistry*; John Wiley and Sons, Inc., New York. 681 pp.

Walters, R. W. and Luthy, R. G. 1984. *Environ. Sci. Technol.* **18**, 395. *As cited in Gustafsson et al., 1997.*

Wolfe, D. A., E. R. Long, G. B. Thursby. 1996. Sediment toxicity in the Hudson-Raritan Estuary distribution an correlations with chemical contamination. *Estuaries* **19**, 901-912.

Youngblood, W. W. and M. Blumer. 1975. Polycyclic aromatic hydrocarbons in the environment: homologous series in soils and recent marine sediments. *Geochim. Cosmochim. Acta* **38**, 1303-1314.

CHAPTER 4: CONCLUSIONS

Polyethylene devices (PEDs) were found to be useful for the measurement of dissolved HOCs like polycyclic aromatic hydrocarbons (PAHs) in natural waters. These sampling devices allow for the measurement of the "truly dissolved" PAH concentration by accumulating the analytes in proportion to only their fugacities or "fleeing tendencies" from the water. One could imagine the use of such devices for assessing the presence of HOCs in the atmosphere, sediment beds, and other media where HOCs may be present in association with multiple phases. These concentrations are of ecotoxicological concern as they reflect the HOC fraction that is driving uptake by the surrounding organisms.

Working in controlled laboratory conditions, it was found that PEDs equilibrated with dissolved PAHs (phenanthrene and pyrene) on daylong timescales. Since the PEDs were deployed in the field over periods of 2-3 days and the accumulations of the PAHs from the water requires days to weeks to equilibrate, the concentrations reported represent time-averaged results. This time averaging limits the likelihood that a non-representative sample may be collected due to temporal changes in sources (e.g., a nearby oil spill at the time of sampling). It was also found that the polyethylene-water partition coefficients for PAHs were comparable to other organic solvent-water partitioning coefficients. These large coefficients allowed for the measurement of dissolved concentrations as low as 1 pg/L for the more hydrophobic PAHs (e.g., benzo(a)pyrene), while concentrations as low as 400 pg/L were measured for less hydrophobic PAHs (e.g., phenanthrene).

Sampling performed in the lower Hudson Estuary revealed increased concentrations of dissolved pyrene and benzo(a)pyrene between neap and spring tides. These data suggest that resuspension events caused an increase in the dissolved concentrations for PAHs with greater hydrophobicities. However, it was found that the PAH water concentrations that we inferred from the PEDs were not at sorptive equilibrium with the aqueous solution. Predicted PAH water concentrations were closer to the observed values when PAH partitioning to soot was included in the partitioning model. This suggested that soot does sorb PAHs in the aquatic environment. However, even when soot was included in the model, the suspended solid phase did not fully explain the discrepancies between dissolved values expected from suspended solid concentrations and observed dissolved concentrations. This suggested that the suspended solids remained in the Hudson River water column for too little time (hours) to complete sorbate transfers to the water sufficient to achieve equilibrium.

Using ratios of source-indicative PAHs, it was estimated that 90% of the dissolved PAH fraction was derived from petrogenic sources. Interestingly, the same ratios indicated that only 55% of the total PAHs (dissolved and sorbed) were from petrogenic sources. As this petrogenically-derived source appears to be more immediately available for uptake by the surrounding biota, it may be prudent for regulatory agencies to focus first on limiting the inputs of petrogenic PAHs. This apparent enhanced solubility for PAHs from petrogenic sources suggests that petrogenically polluted areas are of greater ecotoxicological concern and should be mitigated before areas with predominantly pyrogenically-derived PAHs, which appear to be more strongly sorbed and of less ecotoxicological concern. However, the apparent propensity for oil-derived PAHs to dissolve make

the clean-up of sediments contaminated with such PAHs difficult as many of the PAHs will likely desorb when and if they are disturbed.